RSC Advances

REVIEW

View Article Online
View Journal | View Issue

Cite this: *RSC Adv.*, 2017, **7**, 26226

A review of Mn-containing oxide catalysts for low temperature selective catalytic reduction of NO_x with NH_3: reaction mechanism and catalyst deactivation

Shengen Zhang, * Bolin Zhang, Bo Liu and Shuailing Sun

Atmospheric pollutants of nitrogen oxides (NO_x) can be reduced by selective catalytic reduction (SCR). SCR of NO_x with ammonia (NH_3) at low temperatures has attracted much interest for high nitric oxide (NO) conversion, and this method is dominated by catalysts. Manganese (Mn)-containing oxide catalysts exhibit high activity and selectivity for the unique redox property of manganese oxides (MnO_x). The reaction mechanisms and deactivation processes are summarized in this review. SCR of NO_x with NH_3 follows both the Langmuir–Hinshelwood and the Eley–Rideal mechanisms, which also contribute to the nitrous oxide formation. Fast SCR has a higher reaction rate than standard SCR. Mn-containing catalysts could also be deactivated by sulfur oxides and water vapor. The deactivation process of sulfur dioxide can be classified into two categories: deposition of $(NH_4)_2SO_4$ and sulfation of active sites. The deactivation caused by water vapor can be attributed to the competitive adsorption. The adsorption of water on catalysts' surface blocked the active sites, which are provided for the adsorption of NH_3 and NO. Alkali, alkaline earth and heavy metal ions existing in fine fly ash can also damage the catalysts' acid sites. A notable improvement on performance was obtained when Mn-containing catalysts were doped with a transition metal, for these enhanced its adsorption capacity and oxidation ability. Furthermore, this review gives a comprehensive discussion of the synergistic mechanism between bi-metal or multi-metal oxides. Major conclusions and several possible directions for further research are presented finally.

Received 23rd March 2017
Accepted 27th April 2017

DOI: 10.1039/c7ra03387g

rsc.li/rsc-advances

1. Introduction

Nitrogen oxides (NO_x) are a series of active gases, and include nitrogen dioxide (NO_2), nitrogen oxide (NO) and nitrous oxide (N_2O), and so on. Human activities cause a huge emission rate of NO_x, which is double that of the biotic and abiotic nitrogen fixation rates. Released NO_x can cause a series of environmental issues, such as photochemical smog, acid rain, and ozone depletion, and it can affect global tropospheric chemistry.[1–4] Great efforts have been devoted to abating the emission of NO_x.

The technologies used to control NO_x emission can be categorized as combustion controls and post-combustion controls.[5,6] Combustion controls, which aim to control the production of NO_x, include low NO_x burners,[7] air graded burning and staged fuel combustion.[8] Post-combustion controls aim to decrease the NO_x produced by reducing active N to fixed nitrogen gas (N_2). The technologies for reducing NO_x from flue gas can be divided into: direct decomposition,[9,10] selective catalytic reduction (SCR),[11,12] selective non-catalytic reduction (SNCR),[13,14] hybrid SNCR/SCR[15] and NO_x storage-reduction catalysis.[16] With the advantages of high efficiency and low cost, NO_x emitted from stationary sources (*e.g.*, thermal plants or industrial boilers) has been predominantly controlled by SCR of NO with ammonia (NH_3-SCR) in the presence of excess oxygen (O_2) for decades.[17]

The catalyst to be used is a decisive factor in the process of decreasing NO_x ($deNO_x$). The common catalysts include noble metal catalysts,[18] metal-exchanged zeolite catalysts,[19] metal oxide catalysts,[20,21] heteropoly acid catalysts,[22] and so on. Metal oxide catalysts are widely applied in NH_3-SCR. Nowadays, the most widely used catalysts are vanadium(v)-based catalysts and tungsten trioxide (WO_3) and/or molybdenum trioxide (MoO_3) doped vanadium(v) oxide (V_2O_5)/titanium dioxide (TiO_2) catalysts. These are usually installed at the upstream of flue gas because they require a higher working temperature of 300–400 °C.[23] However, some tough problems have not been solved, such as the effect of excessive dust pollution to the catalysts upstream of the flue, the deactivation by sulfur dioxide (SO_2) and alkali metal ions, the poor thermal stability at high temperatures and the toxicity of vanadium from the disabled catalysts.[24] One of the efficient ways to overcome these obstacles is transferring the SCR reactor from upstream to downstream of

Institute for Advanced Materials and Technology, University of Science and Technology Beijing, Beijing 100083, PR China. E-mail: zhangshengen@mater.ustb.edu.cn

the flue gas, where there is relatively less dust and sulfur oxides in the flue gas but a lower temperature below 300 °C.[25]

A series of metal oxide catalysts have been investigated to adapting low temperature, such as cerium (Ce), cobalt (Co), copper (Cu), iron (Fe), manganese (Mn), molybdenum (Mo), nickel (Ni) and V.[26–30] Of these, manganese oxides (MnO_x) catalysts show a notable NO conversion and N_2 selectivity for its multi oxidation state, high valence state and characteristic crystallinity. Peña *et al.*[26] advocated that MnO_x/TiO_2 had the highest activity among Co, chromium (Cr), Cu, Fe, Mn, Ni and V oxides supported on TiO_2 at low temperatures. Manganese dioxide (MnO_2) and manganese(III) oxide (Mn_2O_3) show the highest activity and N_2 selectivity, respectively, among several MnO_x.[31] The activity and poison tolerance can be improved by doping with other transition metals. Ceria (CeO_2) provides sufficient oxygen in the reaction of redox NO_x, and improves the activity of MnO_x catalysts.[32–34] Mn–Fe spinel shows an excellent SCR performance at low temperature.[35] Other Mn containing catalysts, such as MnO_x–CoO_x/TiO_2,[28,36] MnO_x–CrO_x/TiO_2,[37,38] MnO_x–CuO_x,[39,40] lanthanum manganite ($LaMnO_3$),[41] have been investigated by many researchers. Mn containing catalysts have been recognized as the potential alternative for industrial applications.

To date, advances in low temperature NH_3-SCR of NO_x have been reviewed.[5,6,42] A review by Li *et al.*[43] summarized the use of metal oxides and zeolite catalysts and focused on the catalysts' components, preparation process and catalytic performance, however, the reaction mechanisms were not clarified clearly. A recent review in 2016 by Liu *et al.*[44] summarized the use of MnO_x-based catalysts and concentrated on the technological processes and improvement methods, however, little effort was made to summarize the reaction mechanisms and catalyst deactivation processes.

In this review, the advances in the use of Mn containing oxide catalysts are summarized. The focal point of this review is to address the reaction mechanisms and deactivation processes of Mn containing oxide catalysts. The N_2 selectivity and side reactions are discussed together. This review gives a comprehensive discussion of the synergistic effects between bi-metal or multi-metal oxides. The deactivation process using sulfur oxides, water vapor, alkali metal and heavy metal ions and the regeneration methods are summarized. Finally, the major conclusions and several possible directions of research are presented.

2. Reaction mechanisms

To meet the newest and stringent emission standards, (NO_x concentration $\leq$ 50 mg m^{-3}),[45] academic researchers and engineers are more interested in use of low temperature SCR, which is one of the efficient ways to install a processor downstream of the flue. A number of metal oxide catalysts have been investigated so far. Transition metal oxides play an important role in low temperature SCR catalysts, such as V_2O_5, MnO_x, CeO_2 and copper oxide (CuO). Of these, MnO_x shows an excellent performance because of its different crystallinity, special surface area and multi oxidation. It is vital to elucidate the reaction mechanisms for future research. In this section, the reaction mechanisms of NH_3-SCR over Mn-containing oxide catalysts are summarized.

2.1 Standard SCR

The NH_3-SCR of NO aims to reduce active N to fixed N_2, which is harmless to the atmosphere. In the presence of excess O_2, the main overall reaction is eqn (1).[46] A great number of studies have proposed that eqn (1) shows the reaction stoichiometry in typical SCR conditions.[47–50] In the absence of O_2, reaction in eqn (1) would convert into the reaction in eqn (2):[51]

$$4NH_3 + 4NO + O_2 \rightarrow 4N_2 + 6H_2O(g),\ \Delta G^0_{298} = -1651\ \text{kJ mol}^{-1} \quad (1)$$

$$4NH_3 + 6NO \rightarrow 5N_2 + 6H_2O(g),\ \Delta G^0_{298} = -1821\ \text{kJ mol}^{-1} \quad (2)$$

Because the content of NO is more than 90% among NO_x, eqn (1) is proposed as the standard SCR reaction and dominates the reaction stoichiometry. It is reported widely that the NH_3-SCR of the NO reaction when comparing the stoichiometric conditions follows both the Langmuir–Hinshelwood (L–H) mechanism and the Eley–Rideal (E–R) mechanism.[52,53] Through the L–H mechanism, both NH_3 and NO are adsorbed on the surface of catalysts. However, *via* the E–R mechanism, adsorbed NH_3 reacts with gaseous NO. It is suggested that the gaseous NH_3 could be adsorbed on both Lewis acid sites and Brønsted acid sites, however, the gaseous NO is mainly adsorbed by a physical adsorption process.[54] The adsorption of NH_3 has been recognized as the first step of the SCR reaction because it is easier for NH_3 to be adsorbed on acid sites rather than NO, O_2 and the reaction products.[55]

The SCR process over MnO_x catalysts *via* the L–H mechanism can be approximately described as follows:[23,53,56]

$$NH_3(g) \rightarrow NH_3(ad) \quad (3)$$

$$NO(g) \rightarrow NO(ad) \quad (4)$$

$$Mn^{n+}{=}O + NO(ad) \rightarrow Mn^{(n-1)+}{-}O{-}NO \quad (5)$$

$$NH_3(ad) + Mn^{(n-1)+}{-}O{-}NO \rightarrow Mn^{(n-1)+}{-}O{-}NO{-}NH_3 \rightarrow Mn^{(n-1)+}{-}OH + N_2 + H_2O \quad (6)$$

$$Mn^{(n-1)+}{-}OH + 1/4O_2 \rightarrow Mn^{n+}{=}O + 1/2H_2O \quad (7)$$

Eqn (3) and (4) are the adsorption of gaseous NH_3 and NO. NH_3 is usually adsorbed on the Lewis acid sites and Brønsted acid sites to form adsorbed NH_3 species of coordinated NH_3 and ionic NH_4^+, respectively.[57] Nevertheless, the coordinated NH_3 on the Lewis acid sites possesses a higher thermal stability than the ionic NH^{4+} on Brønsted acid sites. Manganese cations can provide a great number of Lewis acid sites.[49,58]

Fang *et al.*[59,60] investigated the adsorption of NH_3 on the Mn_2O_3 (222), manganese(II,II) oxide (Mn_3O_4) (211) and MnO_2 (110) surfaces using density functional theory. It is claimed that, with more negative adsorption energy values and the shorter

Table 1 The NO conversion of pure MnO_x[59a]

MnO_x	NO conversion (%)				
Reaction temperature	353 K	373 K	393 K	413 K	433 K
MnO_2	13	14	16	19	21
Mn_2O_3	14	17	37	47	44
Mn_3O_4	18	23	34	44	56

[a] Reaction conditions: [NO] = 720 ppm, [NH_3] = 800 ppm, [O_2] = 3%. (Reprinted with permission from ref. 59. Copyright 2013 Elsevier.)

Mn–N bonds, Mn_2O_3 (222) and Mn_3O_4 (211) surfaces were more active for NH_3 adsorption than the MnO_2 (110) surface, which contributed to a higher performance (Table 1). Kapteijn *et al.*[31] proposed that the highest NO conversion is exhibited by MnO_2, followed by Mn_5O_8, Mn_2O_3 and Mn_3O_4.

The adsorbed NO is oxidized by the high valency state Mn^{n+} cations, (*e.g.*, Mn^{4+}) on the catalysts' surface to form adsorbed monodentate nitrite ($Mn^{(n-1)+}$–O–NO) and the very metal cations are reduced as $Mn^{(n-1)+}$ [eqn (5)]. Furthermore, $Mn^{(n-1)+}$–O–NO reacts with adsorbed NH_3 species to form $Mn^{(n-1)+}$–O–NO–NH_3, which decomposes subsequently to N_2 and water (H_2O) [eqn (6)]. Then, the reduced $Mn^{(n-1)+}$ ions are regenerated by gaseous O_2 [eqn (7)].

The SCR process over MnO_x catalysts *via* the E–R mechanism can be described approximately as follows:[35,48,61]

$$NH_3(g) \rightarrow NH_3(ad) \quad (8)$$

$$NH_3(ad) + Mn^{n+}{=}O \rightarrow NH_2(ad) + Mn^{(n-1)+}{-}OH \quad (9)$$

$$NH_2(ad) + NO(g) \rightarrow NH_2NO \rightarrow N_2 + H_2O \quad (10)$$

$$Mn^{(n-1)+}{-}OH + 1/4O_2 \rightarrow Mn^{n+}{=}O + 1/2H_2O \quad (11)$$

The adsorption of NH_3 on the Lewis acid sites is recognized as the first step of NO reduction *via* the E–R mechanism. Coordinated NH_3 could be deprived of a hydrogen and be activated by the labile oxygen or the lattice oxygen of metal oxides to form an amine (NH_2) species [eqn (9)]. Labile oxygen can be released *via* the change of the valence states of Mn. Activated NH_2 species on the catalysts' surface reacted with gaseous NO to form the most important intermediate of NH_2NO, which subsequently decomposes to N_2 and H_2O [eqn (10)]. Then, the reduced $Mn^{(n-1)+}$ cations could be oxidized by O_2.

Furthermore, the formation of NH_4NO_2 is a typical SCR mechanism for Mn-containing catalysts. Qi and Tang,[56] and Eigenmann *et al.*[62] proposed an amide–nitrosamine type mechanism, which is actually similar to the E–R mechanism. An extra species of NH_4NO_2 was presented in this mechanism. NH_4NO_2 could be decomposed to NH_2NO and H_2O, and is then decomposed to N_2 and H_2O [eqn (12)–(14)]:

$$OH(ad) + NO_2(ad) \rightarrow O(ad) + HNO_2(ad) \quad (12)$$

$$NH_3(ad) + HNO_2(ad) \rightarrow NH_4NO_2(ad) \rightarrow NH_2NO(ad) + H_2O \quad (13)$$

$$NH_2NO(ad) \rightarrow N_2 + H_2O \quad (14)$$

In accordance with the transient eqn (3)–(11), Mn^{3+}–O–NO–NH_3 and NH_2NO are the most important intermediate in the reaction of the L–H mechanism and E–R mechanism, respectively. There is a quite similarity between these two different mechanisms. A comproportionation, (*i.e.*, N^{3+} and N^{3-}, $N^{2+}$and N^{2-}) occurs on both the L–H and E–R mechanism (eqn (6) and (10)).[53,63]

2.2 Fast SCR

A fast SCR reaction of NH_3 with NO + NO_2 over Mn-containing oxide catalysts has been reported. It is suggested that the fast SCR has a higher reaction rate than standard SCR.[64] Fast SCR was firstly investigated by Koebel *et al.*, and Madia *et al.*[65–67] The general reaction can be described as follows:[68,69]

$$4NH_3 + 2NO_2 + O_2 \rightarrow 3N_2 + 6H_2O(g),\ \Delta G^0_{298} = -1412\ \text{kJ mol}^{-1} \quad (15)$$

$$4NH_3 + 2NO + 2NO_2 \rightarrow 4N_2 + 6H_2O,\ \Delta G^0_{298} = -1581\ \text{kJ mol}^{-1} \quad (16)$$

In the presence of O_2, NO can be oxidized by active oxygen to form NO_2 [eqn (17)].[70] Judged by the Gibbs free energy, the reaction shown in eqn (15) does not occur easily and consequently limits the rate of eqn (15) or (16). Mn-containing metal oxide catalysts could catalyze this reaction in some extent:[71,72]

$$2NO + O_2 \rightarrow 2NO_2,\ \Delta G^0_{298} = -70\ \text{kJ mol}^{-1} \quad (17)$$

NO_2 is the difference between fast SCR standard SCR. NO_2 acts as a more efficient oxidizing agent than O_2 in the redox process of the SCR reaction. NO_2 can form surface nitrites and nitrates *via* dimerization:[73]

$$2NO_2 \rightarrow N_2O_4 \quad (18)$$

$$N_2O_4 + H_2O \rightarrow HNO_2 + HNO_3 \quad (19)$$

NH_4NO_3 is formed by the reaction between NH_3 and HNO_3. NH_4NO_3 or its related surface species is the key intermediate in the fast SCR process. The reaction processes can be described as follows:

$$2NH_3 + 2NO_2 \rightarrow N_2 + NH_4NO_3 + H_2O \quad (20)$$

$$NH_4NO_3 + NO \rightarrow N_2 + NO_2 + 2H_2O \quad (21)$$

Many researchers considered that NH_4NO_3 would be solid below 170 °C. NH_4NO_3 could be reduced by NO at a higher temperatures [eqn (21)].[64,74] It is pointed out that NH_3 can restrain fast SCR by inhibiting the formation of NO_2 at 150–170 °C.[75] Actually, eqn (21) can be described as two intermediate reactions:

$$NH_4NO_3 \leftrightarrow NH_3 + HNO_3 \quad (22)$$

$$2HNO_3 + NO \rightarrow 3NO_2 + H_2O \quad (23)$$

There is a chemical equilibrium in the fast SCR process [eqn (22)]. The formation of HNO_3 will be restrained while the NH_3 concentration is raised, and that inhibits the formation of NO_2 [eqn (23)]. Among the fast SCR processes, the vital process is the redox reaction between NO and HNO_3, which dominates the rate of fast SCR.

The performance of low temperature SCR has been extensively investigated. Excellent NO conversion and N_2 selectivity has been observed using simulated flue gas in the laboratory. Qi and Yang[76] obtained more than 99% of NO conversion on the $MnO_x(0.3)$–CeO_2 catalyst sintered at 120 °C. Long *et al.*[77] investigated the Fe–Mn-based catalysts. These catalysts showed nearly 100% NO conversion at 100–180 °C. Recently, France *et al.*[78] studied the CeO_2 modified $FeMnO_x$ catalysts, and more than 95% NO conversion was obtained at 90–135 °C without the influence of SO_2 and H_2O. Zhu *et al.*[79] studied the holmium (Ho) modified Fe–Mn/TiO_2 catalysts, which revealed good performance for NO conversion and high SO_2 tolerance. However, more attempts need to be made to understand the fundamental mechanism of low temperature SCR, such as surface chemistry, crystal structure, kinetics and scientific reaction mechanism. These have a great influence on the performance of catalysts and knowledge of them would be beneficial in designing a new catalyst.

2.3 Side reactions

As the reductant, NH_3 is a vital resource in the SCR reaction. NH_3 is consumed mainly *via* N_2 and N_2O formation and the oxidation of the catalyst to NO_x.[52] The wastage of NH_3 is a huge additional cost of the deNO_x process. To decrease the wastage of NH_3, an appropriate NH_3/NO ratio is necessary. Authors agree that a NH_3/NO ratio near to 1 is good. Furthermore, undesired reactions can occur during the SCR process. Eqn (24) and (25) show the undesired ammonia loss:

$$4NH_3 + 4O_2 \rightarrow 2N_2O + 6H_2O(g),\ \Delta G^0_{298} = -1102\ \text{kJ mol}^{-1} \quad (24)$$

$$4NH_3 + 3O_2 \rightarrow 2N_2 + 6H_2O(g),\ \Delta G^0_{298} = -1310\ \text{kJ mol}^{-1} \quad (25)$$

These are the thermodynamically favored reactions but they occur rarely in practice.[80] In addition, there is another undesired reaction during the NH_3-SCR process:

$$4NH_3 + 5O_2 \rightarrow 4NO + 6H_2O,\ \Delta G^0_{298} = -964\ \text{kJ mol}^{-1} \quad (26)$$

Wang *et al.*[81] claim that eqn (26) may replace eqn (1) as the dominant reaction over MnO_x/TiO_2 catalysts when the temperature was raised higher than 175 °C. This was proved by the determination of the components of outlet flue gas. This oxidization of NH_3 gives a decline in NO conversion and extra consumption of NH_3.

When the concentration of NH_3 is appropriate, the formation of N_2O is the primary waste of NH_3 and this decreases the N_2 selectivity [eqn (27)].[35]

$$4NH_3 + 4NO + 3O_2 \rightarrow 4N_2O + 6H_2O(g),\ \Delta G^0_{298} = -1240\ \text{kJ mol}^{-1} \quad (27)$$

Adsorbed NH_3 is oxidized on the catalyst surface to form an amine species (NH_2), which subsequently reacts with NO to form N_2 and H_2O. However, when a further hydrogen atom is abstracted from NH_2 to form an NH species, a N_2O species will be formed by the reaction of the NO and NH species.[82] Both the L–H mechanism and the E–R mechanism pathways contribute to N_2O formation.

As previously mentioned, in the L–H mechanism, physically adsorbed NO can be oxidized by Mn^{n+} to $Mn^{(n-1)+}$–O–NO, which can be further oxidized to monodentate nitrate ($Mn^{(n-1)+}$–O–NO_2) [eqn (28)]. The $Mn^{(n-1)+}$–O–NO_2 can react with adsorbed NH_3 to form $Mn^{(n-1)+}$–O–NO_2–NH_3. Subsequently, $Mn^{(n-1)+}$–O–NO_2–NH_3 will be decomposed to N_2O [eqn (29)]:[17,83]

$$Mn^{(n-1)+}\text{–O–NO} + (1/2)O_2 \rightarrow Mn^{(n-1)+}\text{–O–}NO_2 \quad (28)$$

$$Mn^{(n-1)+}\text{–O–}NO_2 + NH_3(ad) \rightarrow Mn^{(n-1)+}\text{–O–}NO_2\text{–}NH_3 \rightarrow Mn^{(n-1)+}\text{–OH} + N_2O + H_2O \quad (29)$$

As previously mentioned in Section 2.2, the reaction of NH_4NO_3 with NO is a vital step in the fast SCR process. Zhu *et al.*[74] speculated that NH_4NO_3 could be decomposed to N_2O and H_2O *via* the L–H mechanism [eqn (30)]. Referring to eqn (28) and (29), the formation of N_2O could be attributed to the better capacity for NH_3 activation and adsorbed active nitrate species.

$$NH_4NO_3 \rightarrow N_2O + 2H_2O \quad (30)$$

As mentioned previously, in the E–R mechanism, NH_2 species can react with gaseous NO to form N_2 and H_2O. While the NH_2 species is further oxidized on the metal cation to NH species, N_2O will be formed by the reaction of the NH species and gaseous NO [eqn (31) and (32)].[55,63,84] It is obvious that the formation of NH_2NO is a crucial step of NO reduction, which is directly related to the NO conversion and N_2 selectivity.[58]

$$NH_2 + Mn^{n+}{=}O \rightarrow NH + Mn^{(n-1)+}\text{–OH} \quad (31)$$

$$NH + NO(g) \rightarrow N_2O + H^+ \quad (32)$$

Whether the adsorbed NO is oxidized to monodentate nitrate or the NH_2 species is dehydrated to NH, the N_2 selectivity will be restrained and N_2O is formed.[85] This is an important difference from the standard SCR. The formation of N_2 and N_2O during the SCR process is illustrated in Fig. 1.

Hinted at by the previous equations, it is obvious that the two N atoms in N_2O originate from NO and NH_3, respectively. Suárez *et al.*[86] pointed out that N_2O did not primarily originate from the NH_3 oxidation reaction. The feasible main reaction path is that between the coordinated NO_3^- (generated from NO/

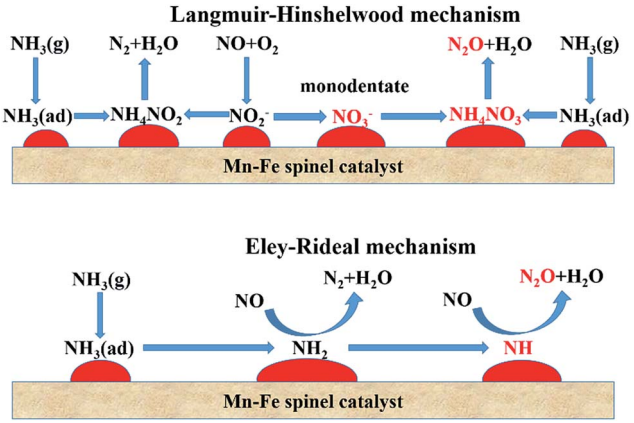

Fig. 1 The scheme of the SCR reaction through L–H and E–R mechanisms over Mn–Fe spinel catalyst. (Reprinted with permission from ref. 35. Copyright 2014 American Chemical Society.)

NO_2 in the presence of O_2) and the adsorbed NH_x. Tang *et al.*[63] demonstrated that the N_2O selectivity of the SCR reaction over β-MnO_2 was higher than that over α-Mn_2O_3 at 150 °C. The N_2O is generated directly from the reaction of NO with NH_3 *via* the E–R mechanism. Use of calcium (Ca) modification improves the performance of N_2 selectivity for Mn-containing catalysts.[87]

It is suggested that N_2O formation mainly resulted *via* the E–R mechanism.[53] Yang *et al.*[35] studied the mechanism of N_2O formation over Mn–Fe spinel catalysts. N_2O formation *via* the E–R mechanism was much more than *via* the L–H mechanism over the Mn–Fe spinel catalysts. In addition, N_2O selectivity was not promoted by increasing the NO concentration, but it was increased with the increase in NH_3 concentration. N_2O selectivity is also related to the gas hourly space velocity (GHSV). It was also found that N_2O in the SCR reaction over Mn–Ce catalysts was generated *via* the E–R mechanism, not the L–H mechanism.[88] The choice of E–R or L–H mechanisms ways will vary with the changes of temperature. It is reported that the L–H mechanism plays the main role below 150 °C, and the E–R mechanism way dominates the SCR reaction at higher temperatures.[55,89]

2.4 Synergistic effect

A pure metal oxide may not be suitable for practical applications because of its defects. However, the property of one metal oxide can be improved by introducing foreign metal cations into its lattice. There will also be an interaction between different metal oxides. For example, reports in the literature indicate that Mn–Ce mixed oxide catalysts demonstrated the best performance among a multitude of metal oxide catalysts. Ceria can enhance the adsorption of NO and O_2, which benefits the oxidation of NO to NO_2 and improve sulfur resistance. Qi and Tang[76] found that the oxidation of NO to NO_2 was increased significantly after addition of ceria to MnO_x and that it speeded up the overall process. Actually, pure CeO_2 cannot be applied in industry because of its small specific surface area and low thermal stability.[90] Meanwhile, as is reported,[91] modification with titanium (Ti) or tin (Sn) can improve the SCR property of cerium oxides. Qi *et al.* and Imamura *et al.*[27,92] found using X-ray diffraction patterns that there was no manganese oxide phase in the calcined Mn–Ce catalyst prepared by a co-precipitation method. This indicated that strong interactions exist between manganese and cerium oxides, because Mn_2O_3 and MnO_2 can be detected in pure manganese oxide calcined at the same temperature.

The redox property of catalysts is the key factor of the NH_3-SCR processes.[29] Electronic transfer, showing as oxidation and reduction, plays quite an important role in catalytic reactions. The redox couples exist over the metal oxide catalysts, such as Mn^{4+}/Mn^{3+}, Ce^{4+}/Ce^{3+} and Fe^{3+}/Fe^{2+}, which provide the redox cycles with excess oxygen. The activity of bi-metal and multi-metal oxide catalysts could be promoted by dual redox cycles. The general formula can be described as follows:

$$M^{n+} + N^{m+} \leftrightarrow M^{(n-1)+} + N^{(m+1)+} \quad (33)$$

There is a typical SCR reaction process *via* the E–R mechanism on Mn–Ce/TiO_2 and Mn–Ce/aluminium oxide (Al_2O_3) catalysts.[27,93] Manganese oxides and ceria oxides also interact. They can form a solid solution because of the similarity of their structure.[94] Ceria has a superior oxygen storage performance. Thus, the process of oxidizing Mn^{3+} to Mn^{4+} is enhanced by using ceria.[95]

Liu *et al.*[96] investigated a Mn–Ce–Ti mixed oxide catalyst prepared using a hydrothermal method, and found that there were dual redox cycles, such as $Mn^{4+} + Ce^{3+} \leftrightarrow Mn^{3+} + Ce^{4+}$ and $Mn^{4+} + Ti^{3+} \leftrightarrow Mn^{3+} + Ti^{4+}$. These dual redox cycles can promote each other and facilitate the electron transfer between Mn, Ce and Ti active sites by decreasing the migration energy. The proposed schemes are as follows (Fig. 2).

The scheme shows that Mn cation sites may be the main active site for the adsorption of N. Furthermore, the addition of Ce, Fe, Cu, Ni and so on, may show a synergistic effect, which

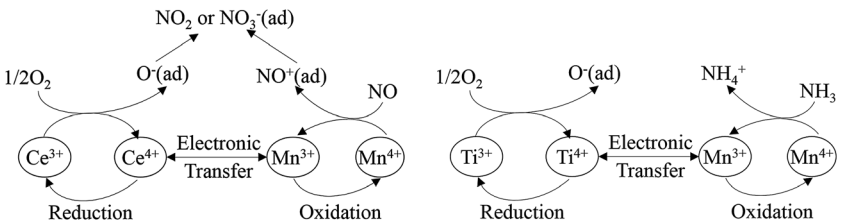

Fig. 2 The scheme of dual redox cycle during SCR process. (Reprinted with permission from ref. 96. Copyright 2014 American Chemical Society.)

facilitates the generation of Mn^{4+} from Mn^{3+}. Kwon *et al.*[97] studied the MnO_x/CeO_2–TiO_2 catalyst system. When Ce was added to Mn/Ti, an oxygen bridge of Mn–O–Ce was formed and, thus enhanced the binding between Mn and O_2. This oxygen bridge provided a channel for the electron transfer between manganese and cerium cations, and particularly accelerated the oxidation of Mn^{3+} to Mn^{4+} by Ce^{4+}.[23]

$$Mn_2O_3 + 2CeO_2 \rightarrow 2MnO_2 + Ce_2O_3 \quad (34)$$

Among the Mn–Fe mixed oxide catalysts, electronic transfer occurs between the different oxidation states of Fe^{3+}, Fe^{2+}, Mn^{4+} and Mn^{3+}.[98] The performance of the Mn/TiO_2 catalyst was improved by the addition of Fe.[99] The process can be described approximately as follows:

$$Fe^{3+} + Mn^{3+} \leftrightarrow Fe^{2+} + Mn^{4+} \quad (35)$$

$$NO + Mn^{4+} \rightarrow NO^+(ad) + Mn^{3+} \quad (36)$$

$$1/2O_2 + Fe^{2+} \rightarrow Fe^{3+} + O^-(ad) \quad (37)$$

$$NO^+(ad) + O^-(ad) \rightarrow NO_2 \quad (38)$$

$$\equiv Fe^{2+} + \equiv Mn^{4+} \rightarrow \equiv Fe^{3+} + \equiv Mn^{3+} \quad (39)$$

Liu *et al.*[100,101] investigated a series of WO_3-doped Mn–zirconium (Zr) mixed oxide catalysts. Using catalyst performance measurements, the SCR performance and poisoning tolerance of the Mn–Zr catalyst doped with WO_3 was higher than that for the Mn–Zr catalyst alone. There were redox couples of Mn^{4+}/Mn^{3+} and W^{6+}/W^{5+}, (*i.e.*, $W^{5+} + Mn^{4+} \leftrightarrow W^{6+} + Mn^{3+}$). The redox property and the electron transfer was improved using these dual redox couples (Fig. 3). Thus, the electron transfer between Mn and W active sites was promoted and this contributes to the activation of NH_3 and an improvement of the NO conversion (Fig. 4).

Metal oxides could catalyze the reduction of NO with NH_3 *via* the transfer of electrons.[102,103] As is known, catalysts play a role in accelerating the reaction rate. Referring to Fig. 2, it can be seen that metal cations provide the adsorption sites and function as the transfer station of electrons in the SCR process. Manganese mainly acts as the adsorption center for nitrogen. Mn^{4+} receives an electron from NO or NH_3 and will be reduced into Mn^{3+}. Then the reduced Mn^{3+} would be restored to Mn^{4+} by an extra oxygen and then the next redox cycle starts. However, a faster pathway is *via* the transfer of an electron between metal oxides, such as Ce, Fe, W and so on. Therefore, to design a catalyst, it is necessary to introduce an element for the role of the adsorption and oxidation of nitrogen. Simultaneously, another element is required for superior oxygen storage to quickly restore the reduced element. The coordination of these two types of elements will improve the performance of SCR.

It is essential to characterize the catalysts' structure in order to design an excellent catalyst. The current technology for treating the exhaust gas is supported vanadium-based catalysts

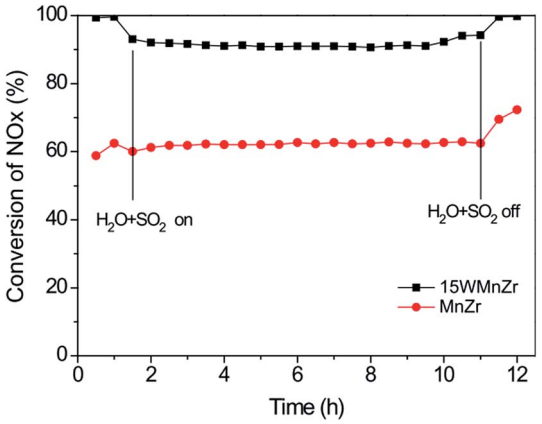

Fig. 4 NO_x conversion over MnZr and WMnZr catalysts at 300 °C. Reaction conditions: [NO] = [NH_3] = 500 ppm, [O_2] = 5%, [H_2O] = 5%, [SO_2] = 50 ppm, GHSV = 128 000 h^{-1}. (Reprinted from ref. 100. Copyright 2015, with permission from Elsevier.)

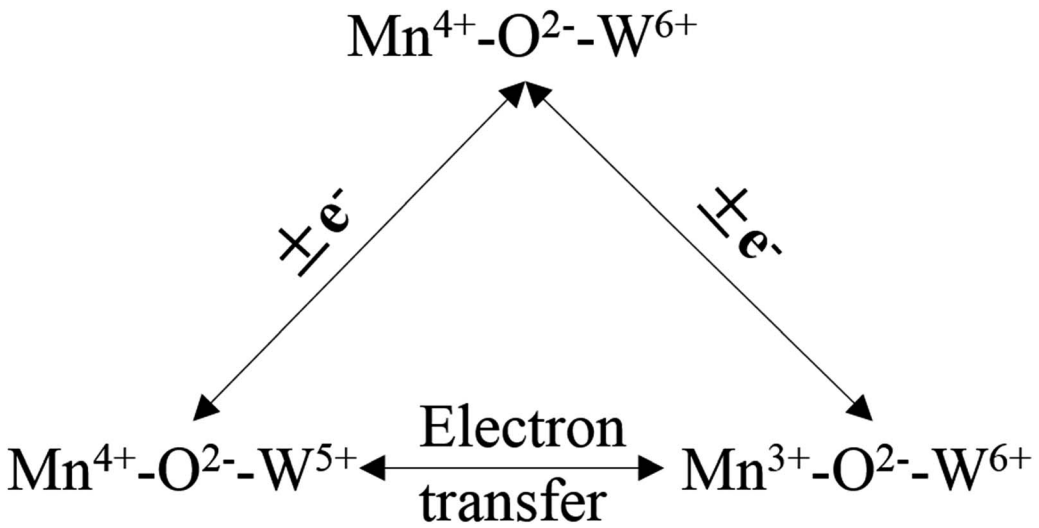

Fig. 3 The electron transfer of redox couples of Mn^{4+}/Mn^{3+} and W^{6+}/W^{5+}.

Table 2 Brunauer–Emmett–Teller (BET) surface area and TOF of different loadings of Mn/TiO_2 catalysts[106a]

Catalyst	BET surface area ($m^2\ g^{-1}$)	TOF at different GHSV (h^{-1})	
		50 000	100 000
5% Mn/TiO_2	238	139.5	127.8
11.1% Mn/TiO_2	229	60.1	58.7
16.7% Mn/TiO_2	196	32.3	31.7
20% Mn/TiO_2	183	27.8	27.5
24% Mn/TiO_2	165	22.0	21.3

[a] Reprinted with permission from ref. 106. Copyright 2007 Elsevier.

on TiO_2 modified by W or Mo addition. Depending on the coverage, different polymeric vanadium oxides (VO_x) could segregate at the surface and these exhibited different turnover frequency (TOF) and selectivity.[104,105] This could be interesting if the same trend existed for MnO_x species, however, there has been little research proposed on use of different polymeric MnO_x corresponding to their different performances. Ettireddy *et al.*[106] studied TiO_2 supported manganese oxide catalysts. Different TOFs were obtained on the Mn/TiO_2 loaded with different amounts of manganese (Table 2). It was proposed that the polymeric or microcrystalline form of MnO_x was envisaged at higher loadings. As a general trend, the TOF and selectivity decreased with the polymeric form increasing at higher loadings. However, further study should be done to confirm which kind of polymeric manganese was formed and its TOF and selectivity should also be determined.

In this section, the reaction mechanisms have been summarized. It was supposed originally that NO_2 could be the reactant of SCR process. However, it is widely agreed that the main reactant for the SCR process is NO, while NO_2 is reduced by the fast SCR process.[107] The synergistic effect among the different metal cations is essential to improve the catalysts' performance, such as NO conversion, selectivity and poisons' tolerance. According to various reports, the low resistance to different poisons is the greatest obstacle for the application of low temperature SCR catalysts.

3. Catalyst deactivation

Because of the demands of high temperature operation, conventional SCR catalysts suffer a huge amount of damage from the sulfur oxides, water vapor, heavy metal ions and alkali and alkaline earth metal ions in the upstream of the flue gas.[108] Installing the reactor downstream of the desulfurizer and precipitator is an excellent way to avoid deactivation. Many metal oxide catalysts have been reported as being low temperature SCR catalysts,[99,109,110] however, commercial low temperature SCR catalysts have narrow fields of application because they are not immune to the residual SO_2 and H_2O contained in real flue gas. The poor tolerance of SO_2 and H_2O has been a major obstacle for practical applications.[111] Therefore, it is significant to illuminate the poisoning mechanisms of SO_2, H_2O and so on.

3.1 SO_2 and H_2O

Sulfur oxides are mainly generated from the combustion of fossil fuels and the sintering of ore. Residual SO_2 after desulfurization can still damage the metal oxide catalysts. The deposition of ammonium sulfates, such as ammonium bisulfate (NH_4HSO_4) and ammonium sulfate [$(NH_4)_2SO_4$], is the primary cause for the deactivation of metal oxide catalysts at low temperature.[112] The decomposition temperature of ammonium sulfite [$(NH_4)_2SO_3$] and $(NH_4)_2SO_4$ salts is higher than the operation temperature of the catalysts. Most researchers regard the poisoning of SO_2 as a major problem. The deactivation of SO_2 can be classified into two categories: deposition of $(NH_4)_2SO_4$ and sulfation of active sites. The undesired metal sulfates and $(NH_4)_2SO_4$ would occupy active sites on the surface and gradually deactivate the catalyst. The deactivation caused by water vapor can contribute to the competitive adsorption. The adsorption of H_2O on the catalysts' surface blocks the active sites, which are provided for the adsorption of NH_3 and NO.

3.1.1 Deposition of ammonium sulfates. The harm caused by $(NH_4)_2SO_3$ and $(NH_4)_2SO_4$ is to mainly block the active sites. The micropore surface area and volume was decreased after SO_2 was introduced in to a simulated flue gas.[113] When excess O_2 exists in the flue gas, the trace residual SO_2 can be oxidized to SO_3, a reaction catalyzed by the metal active sites [eqn (34)]. Furthermore, it was proved that the SO_2 could be easily oxidized on the MnO_x catalysts' surface. Also, NO_x would further facilitate the oxidation of SO_2 to SO_3 [eqn (35)].[111] The reaction could be described approximately as follows:

$$SO_2 + 1/2O_2 \rightarrow SO_3 \quad (40)$$

$$NO_2 + SO_2 \rightarrow NO + SO_3 \quad (41)$$

Gaseous NH_3 was assisted by the Brønsted acid sites to form NH_4^+, which could react with SO_2 or SO_3 to form $(NH_4)_2SO_3$ or $(NH_4)_2SO_4$, respectively. In addition, NH_4HSO_4 species were also generated in the flue gas. The formation of NH_4HSO_4, $(NH_4)_2SO_3$ and $(NH_4)_2SO_4$ can be described as follows:[114]

$$SO_3 + H_2O \rightarrow H_2SO_4 \quad (42)$$

$$H_2SO_4 + NH_3 \rightarrow NH_4HSO_4 \quad (43)$$

$$2NH_3 + SO_2 + H_2O \rightarrow (NH_4)_2SO_3 \quad (44)$$

$$2NH_3 + SO_3 + H_2O \rightarrow (NH_4)_2SO_4 \quad (45)$$

Actually, $(NH_4)_2SO_3$ and $(NH_4)_2SO_4$ can be decomposed at a relatively higher temperature. However, low temperature SCR of NO_x is usually requested at a low operation temperature, which is lower than the decomposition temperature of the $(NH_4)_2SO_3$ and $(NH_4)_2SO_4$. Therefore, removing the undesired side-products of $(NH_4)_2SO_4$ salts is a big challenge to researchers.

Almost all of reported MnO_x catalysts were affected by the introduction of SO_2 in the feed gas.[115] Zhang *et al.*[116] introduced 100 ppm SO_2 in the feed gas, which induced an apparent

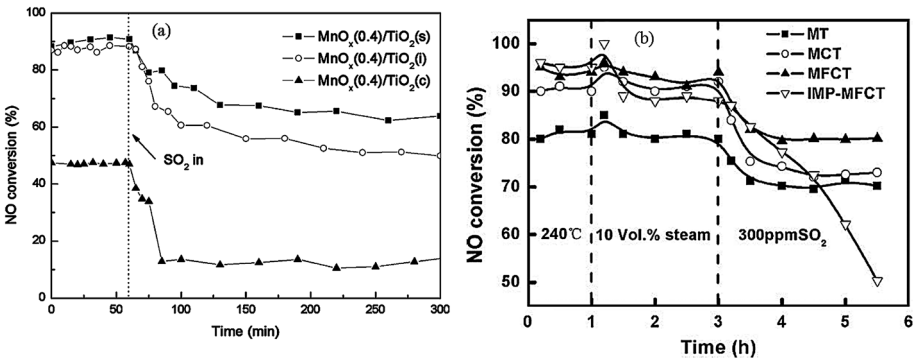

Fig. 5 The effect of SO_2 on NO conversion. (a) Reaction conditions: [NO] = [NH_3] = 1000 ppm, [O_2] = 3%, [SO_2] = 200 ppm, balance N_2, temperature: 150 °C, GHSV = 30 000 h^{-1}. (Reprinted from ref. 118. Copyright 2008, with permission from Elsevier.) (b) Reaction conditions: [NO] = 600 ppm, [NH_3] = 480 ppm, [O_2] = 2%, [SO_2] = 300 ppm, [H_2O] = 10 vol%, balance N_2, temperature: 240 °C, GHSV = 24 000 h^{-1}. (Reprinted from ref. 111. Copyright 2009, with permission from Elsevier.)

decrease of NO conversion over the Mn–Ce metal oxide catalysts supported on carbon nanotubes. Lu *et al.*[117] fed 200 ppm SO_2 to the flue gas, and then the NO_x conversion of Mn–Ce/TiO_2 catalyst decreased from an initial value of 99% to about 78%. Jiang *et al.*[118] investigated the effect of SO_2 on MnO_x(0.4)/TiO_2 catalysts prepared by three methods, sol–gel, impregnation and co-precipitation. The NO conversions had an apparent decrease for these catalysts (Fig. 5a).

Yu *et al.*[111] prepared MnO_2–Fe_2O_3–CeO_2–TiO_2 catalysts. The performance of this catalyst was decreased by introducing SO_2. The NH_4^+ species and the SO_4^{2-} species were determined from Fourier-transform infrared spectra. The NH_4^+ species were chemisorbed on to the Brønsted acid sites.[119] This means that the poisoning of SO_2 can be *via* the formation and deposition of $(NH_4)_2SO_4$, which blocks the active channels of the catalyst. The NO conversion was decreased to 50% from 90% (Fig. 5b).

Xu *et al.*[120] also found that NH_4HSO_3 and NH_4HSO_4 formed *via* the reaction of SO_2 and NH_3 could be deposited on catalysts' surface and blocked the active sites [eqn (34)–(39)]. Furthermore, more Brønsted acid sites will be generated while the sulfates are formed by SO_2 adsorption on surface. The Lewis acid site could be transformed to the Brønsted acid site by adsorption of a water molecule.[121] This means that a wet atmosphere would promote the formation of the Brønsted acid sites, which facilitates the sorption of NH_4^+.[122] In terms of diffuse reflectance infrared Fourier transform (DRIFT) spectra, Jiang *et al.*[123] proved that the formation of NH_4^+ was promoted after introducing SO_2. However, even though Brønsted acid sites were formed by the sulfatization, NO conversion was decreased because SO_2 occupied the NO adsorption sites.

Therefore, to obtain high NO conversion, it is necessary to prevent the formation of $(NH_4)_2SO_4$. Actually, it is nearly impossible to eliminate the residual SO_2 completely. Efficient ways to do it may be preventing the oxidation of SO_2 and decreasing the decomposition temperature of $(NH_4)_2SO_4$ and NH_4HSO_4 on the catalysts' surface.

Jin *et al.*[25] studied the Mn–Ce/TiO_2 and Mn/TiO_2 catalysts. In terms of the thermogravimetry/differential scanning calorimetry (TG/DSC) results, the decomposition temperatures of $(NH_4)_2SO_4$ and NH_4HSO_4 on the Mn/TiO_2 catalyst was determined to be 213 °C and 361 °C, respectively. However, in the case of the Mn–Ce/TiO_2 catalyst, the decomposition temperature of NH_4HSO_4 was approximately 286 °C, which was much lower than 361 °C. This indicated that the thermal stability of NH_4HSO_4 on the catalyst was greatly reduced after introducing cerium. This inference was also proved by the DRIFT results. Therefore, ceria improved the performance of Mn/TiO_2 catalyst.

There is a universal agreement that residual SO_2 damages the metal oxide catalysts and decreases the NO conversion. $(NH_4)_2SO_3$ and $(NH_4)_2SO_4$ were formed on catalysts' surface by the reaction of SO_2. Researchers found that the NO conversion would increase for a while when SO_2 was introduced and then finally decrease. The adsorption of SO_2 improved the amount of Lewis acid sites, and thus the capacity of NH_3 was improved. However, the sulfation damages the manganese cations, which are the active sites of NO.

3.1.2 Sulfation of active sites. The presence of SO_2 could trigger the sulfation of the dominating active phase of metal oxide catalysts. Furthermore, the harm caused by the sulfation would be permanent and irreversible.[124] Jiang *et al.*[123] described a proposed mechanism of SO_2 deactivation effect for a Fe–Mn/Ti catalyst. The scheme in Fig. 6a shows the formation of Lewis acid sites. Mn cations are the active sites for the adsorption of NO to form bidentate or monodentate nitrates (Fig. 6b), however, when both NO and SO_2 exist in the flue gas, NO and SO_2 were adsorbed competitively. The adsorption ability of SO_2 was much higher than that of NO (Fig. 6c), so SO_2 occupied the active sites and the catalyst was sulfated. Furthermore, Fig. 6d shows that NH_3 could be adsorbed on the Lewis acid site of the Mn cations. When the active sites were sulfated, the Lewis acid sites could be transformed to the Brønsted acid sites *via* bonding of a water molecule. Therefore, this did not affect the adsorption of NH_3, because NH_3 could also be adsorbed on the Brønsted acid sites (Fig. 6e). It is therefore, proposed that the effect of SO_2 was mainly on the adsorption of NO rather than on the adsorption of NH_3.

Yu *et al.*[111] investigated the formation of metal sulfation on fresh Mn–Fe–Ce–Ti catalyst impregnated $(NH_4)_2SO_4$. In terms of

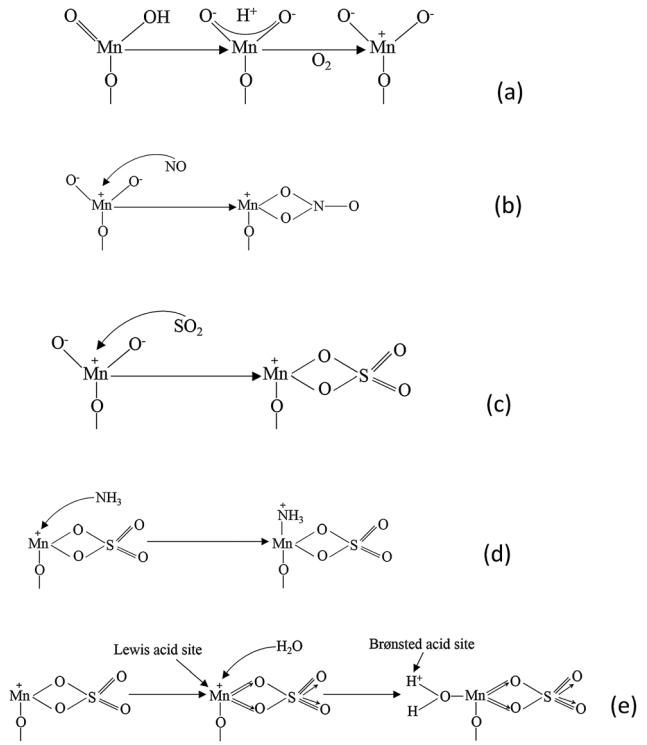

Fig. 6 The proposed mechanism of SO_2 deactivation effect on the SCR reaction. (Reprinted with permission from ref. 123. Copyright (2010) American Chemical Society.)

the TG curve, SO_3 was released from $(NH_4)_2SO_4$ decomposition and then combined with Mn species to form manganese sulfate ($MnSO_4$). They claimed that the $MnSO_4$ could not be formed directly by the reaction of oxidized SO_2 and Mn species.[57] Kijlstra *et al.*[125] proved that the transformation of MnO to $MnSO_4$ on MnO_x/Al_2O_3 catalyst significantly deactivated the catalyst's activity.

Efforts have been made to facilitate the SO_2 tolerance of metal oxide catalysts. Ceria may trap SO_2 for NO_x storage catalysts to limit the sulfation of the dominating active phase and inhibit the formation of $(NH_4)_2SO_4$ and NH_4HSO_4.[117,126] After pre-treatment with SO_2, Ce doped Mn/TiO_2 catalysts had more Lewis acid sites than Mn/TiO_2 catalysts. This result implied that the addition of ceria could prevent the Lewis acid sites from the sulfation of SO_2.

Liu *et al.*[127] compared the performance of Mn–Ce mixed oxide catalysts prepared using the surfactant template method and the conventional co-precipitation method. Referring to the catalytic activity measurement, the Mn_5–Ce_5 catalyst prepared using the surfactant template method showed the highest NO_x conversion whether SO_2 and H_2O were introduced or not. The catalysts prepared using the surfactant template method possessed a higher surface area and smaller active sites, which contributed to a higher NO_x reduction.

In terms of *in situ* DRIFT analysis, Jin *et al.*[25] found that the Lewis acid sites could be preserved effectively with the doping of Ce while the SO_2 was added. SO_2 was oxidized to SO_3 or sulfation species on MnO_x, however, SO_3 and sulfation species move

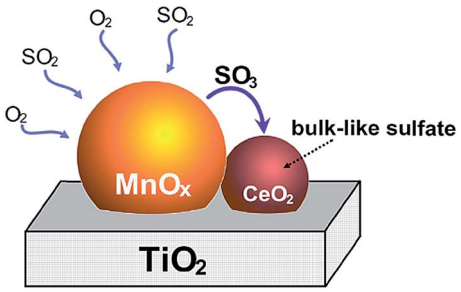

Fig. 7 The formation schematic of bulk like sulfate on Mn–Ce/Ti catalysts. (Reprinted from ref. 25. Copyright 2013, with permission from Elsevier.)

into ceria to form bulk like sulfate species. Therefore, ceria trapped SO_2 and protected the dominant active manganese cations (Fig. 7). Furthermore, in terms of the DRIFT and TG-DSC results, it was indicated that the thermal stability of sulfation species over the Mn–Ce catalyst was lower than that over the MnO_x catalyst. Referring to the study of Kylhammar *et al.*,[128] it is assumed that the bulk sulfation species in ceria reveals a high mobility, which facilitates their desorption.

Wang *et al.*,[113] Xu *et al.*,[120] and Shi *et al.*[129] proved that the active manganese cation was reserved for ceria, which finally sulfated it. Ce^{4+} distributed on the catalysts' surface transformed into Ce^{3+} after sulfation. The reaction can be described as follows:

$$2CeO_2 + 3SO_2 + O_2 \rightarrow Ce_2(SO_4)_3 \quad (46)$$

Furthermore, it is reported that Zr could optimize the redox property and strengthen SO_2 tolerance.[89] Chang *et al.*[130,131] reported that Sn modification could further improve the tolerance of the Mn–Ce catalyst to SO_2 and H_2O. They compared the NO conversion of Sn(0.1)–Mn(0.4)–Ce(0.5)–O and Mn(0.4)–Ce(0.6)–O mixed oxide catalysts. It was obvious that the NO conversion of the Mn(0.4)–Ce(0.6)–O catalyst was decreased more significantly than that of the Sn(0.1)–Mn(0.4)–Ce(0.5)–O catalyst when 200 ppm of SO_2 and 3% O_2 was fed in to the system at 220 °C.

Shi *et al.*[132] compared the resistance of the Mn/TiO_2 catalyst and the hierarchically macro-mesoporous Mn/TiO_2 (HM-Mn/TiO_2) catalyst prepared by the sol–gel method. After feeding 30 ppm SO_2 to the system, the NO conversion of the Mn/TiO_2 catalyst decreased sharply from 57% to 15%, however, the NO conversion of the HM-Mn/TiO_2 catalyst kept a higher value of more than 84%. The result indicated that maybe the SO_2 resistance could be improved by using a hierarchically macro-mesoporous structure.

As previously, because NH_3 could be adsorbed on both the Lewis acid sites and the Brønsted acid sites, there is little influence on the adsorption of NH_3. However, the adsorption ability of SO_2 was higher than that of NO. Residual SO_2 would be adsorbed on Mn cations, which are the active sites for the adsorption of NO. The damage caused by sulfation would be permanent and irreversible. Doping with ceria should be a good choice to divert this damage from Mn. More research should be done to investigate the reaction mechanism between SO_2 and

Mn cations. The correlations should be established between the extent of sulfation and the degree of dispersion of MnO_x species at the surface.

3.1.3 Effect of H_2O. Water vapor could decrease the activity and show a notable inhibition on low temperature SCR. H_2O can be generated from the original flue gas or the reaction of SCR of NO. Even though there is no H_2O in the original flue gas, H_2O vapor will be generated during the SCR reaction, as shown in eqn (1). This means that the presence of H_2O is nearly inevitable. Therefore, many efforts have been made to evaluate the durability of metal oxide catalysts in the presence of H_2O vapor. As mentioned previously, trace SO_2 could still decrease the activity of the metal catalyst. The deactivation process of SO_2 would be enhanced in the case of H_2O vapor.

The main reason for the decrease of activity can be attributed to the competitive adsorption of H_2O. Many researchers reported that the adsorption of H_2O on the catalysts' surface blocked the active sites, which are provided for the adsorption of NH_3 and NO.[109,133] Chen *et al.*[134] studied a MnO_x–niobium oxides (NbO_x)–CeO_2 catalyst prepared by a sol–gel method and found that the adsorption of H_2O inhibited the adsorption of NO_x. Xiong *et al.*[108] compared the SCR performance of Mn–Fe spinel catalysts in the presence and absence of H_2O. They proposed that the effect of H_2O can be attributed to the competitive adsorption, the decrease of oxidation ability and the inhibition of interface reactions.[135,136] The temperature programmed desorption (TPD) profiles of NH_3 and NO_x were obtained, and the NO_x and NH_3 adsorption capacity of Mn–Fe spinel in the absence of H_2O and in the presence of 5% H_2O are shown in Table 3.

Fig. 8 shows that the NO_x conversion apparently decreased when 5% H_2O was fed in to the flue gas, especially at the lower temperature, *e.g.*, below 160 °C. The adsorption of H_2O vapor on the catalyst's active sites deprived the sites of NH_3 adsorption, which apparently decreased the NO conversion. There is a summary of Mn-containing catalysts' performance in the presence and in the absence of SO_2 and H_2O (Table 4).

3.1.4 Regeneration. Many articles reported that the deactivated $(NH_4)_2SO_4$ could be regenerated after use. Water washing, thermal regeneration, thermal reduction regeneration and reductive regeneration were the usual methods to regenerate the deactivated catalysts.[137,149] Yu *et al.*[150] investigated the regeneration of the SCR catalyst using dilute sodium hydroxide solution. The catalyst was deactivated by the deposition of sulfates on the surface. Pourkhalil *et al.*[151] regenerated the deactivated MnO_x catalysts *via* heating at 350 °C for 2 h. This was a reversible process because of $(NH_4)_2SO_4$ salts can be decomposed. Jin *et al.*[25] regenerated the Mn/Ti and Mn–Ce/Ti catalysts with water washing (Fig. 9a). Shi *et al.*[129] regenerated the CeO_2 catalysts using a thermal treatment (Fig. 9b).

Huang *et al.*[152] investigated a series of Fe–Mn oxide catalysts supported on mesoporous silica (MPS), which showed good activity. When H_2O and SO_2 was fed in to the system at 190 °C, the NO conversion over Mn–Fe/MPS was finally decreased to 85.3% from 99.2%. This was attributed to the formation of the NH_4HSO_4 and $(NH_4)_2SO_4$ in the presence of both H_2O and SO_2. However, the deactivated catalyst could be regenerated using a heating treatment, because the deactivation was because of the catalyst pore plugging and surface area loss by the deposition of $(NH_4)_2SO_4$. When the temperature is above 140 °C, H_2O has no negative effect on its activity.

Guan *et al.*[153] investigated the resistance to deactivation by H_2O and SO_2 of $Ti_{0.9}Ce_{0.05}V_{0.05}O_{2-x}$ catalysts, which showed a high NO conversion and N_2 selectivity. After feeding 400 ppm SO_2 for 26 h at 150 °C, the surface of catalyst was deposited with significant agglomeration and bulk NH_4NO_3 and $(NH_4)_2SO_4$ with a size of 30–50 μm. Then, the NH_4NO_3 and $(NH_4)_2SO_4$ was decomposed when the catalyst was calcined at 200 °C and 400 °C, because the decomposition temperatures were 170 °C and 300 °C, respectively. The surfaces were scanned using scanning electron microscopy (SEM), and the transformation of the surface is shown in Fig. 10.

Table 3 Capacity of Mn–Fe spinel for NH_3 and NO_x adsorption at 150 °C μmol^{-1} g^{-1}[108]

Condition	NH_3 (μmol^{-1} g^{-1})	NO_x (μmol^{-1} g^{-1})
In the absence of H_2O	122	82
In the presence of 5% H_2O	105	46

3.2 Alkali and alkaline earth metal ions

Fine fly ash still exists in the downstream of the flue gas after desulfurizing and dedusting. Amounts of alkali and alkaline earth metals were released from the raw materials or coal, such

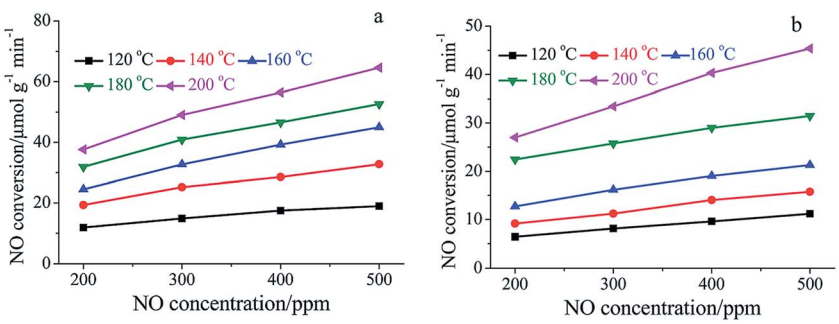

Fig. 8 Dependence of NO conversion rate on gaseous NO concentration over Mn–Fe spinel: (a) in the absence of H_2O; (b) in the presence of 5% H_2O. (Reproduced from ref. 108 with permission from the Royal Society of Chemistry.)

Table 4 Summary of Mn-containing catalysts' performance in the absence/presence of SO_2 and H_2O

Catalysts	Preparation process[a]	Reaction conditions[b]	NO_x conversion 1[c]	Poison condition[d]	NO_x conversion 2[e]	Ref.
$Mn_{0.4}$–$Ce_{0.5}$–$Sn_{0.1}$–O	Co-precipitation/500 °C/6 h	0.1% NO, 0.1% NH_3, 2% O_2/35 000 h^{-1}	100% (110–230 °C)	0.01% SO_2, 9% H_2O	62% (110 °C)	130
$Mn_{0.2}$–$Ce_{0.1}$–$Ti_{0.7}$–O	Hydrothermal/500 °C/6 h	0.05% NO, 0.05% NH_3, 5% O_2/64 000 h^{-1}	>92% (150–250 °C)	0.005% SO_2, 5% H_2O	~90% (200 °C/10 h)	96
$Mn_{0.3}$–$Ce_{0.7}$–O	Citric acid/650 °C/6 h	0.1% NO, 0.1% NH_3, 2% O_2/42 000 h^{-1}	>95% (100–150 °C)	0.01% SO_2, 2.5% H_2O	~95% (120 °C/4 h)	76
Mn_5–Ce_5–O	Surfactant template/500 °C/4 h	0.05% NO, 0.05% NH_3, 5% O_2/64 000 h^{-1}	>95% (100–200 °C)	0.005% SO_2, 5% H_2O	>90% (150–200 °C/-)	127
$Mn_{0.28}$–$Ce_{0.05}$–$Ti_{0.67}$–O	Co-precipitation/400 °C/2 h	0.06% NO, 0.06% NH_3, 3% O_2/40 000 h^{-1}	>92% (120–180 °C)	0.07% SO_2, 3% H_2O	35% (120 °C/13 h)	137
$Mn_{0.4}$–$Ce_{0.07}$–Ti_1–O	Sol–gel/500 °C/6 h	0.08% NO, 0.08% NH_3, 3% O_2/40 000 h^{-1}	~100% (100–180 °C)	0.01% SO_2, 3% H_2O	~60% (100 °C/10 h)	138
$Sn_{0.1}$–$Mn_{0.4}$–$Ce_{0.5}$–O	Co-precipitation/500 °C/6 h	0.1% NO, 0.1% NH_3, 2% O_2/35 000 cm^3 g^{-1} h^{-1}	~100% (110–230 °C)	0.01% SO_2, 12% H_2O	~70% (110 °C/9 h)	131
Mn_1–$Ce_{0.3}$/TiO_2–graphene	Impregnation/500 °C/6 h	0.05% NO, 0.05% NH_3, 7% O_2/67 000 h^{-1}	>90% (140–180 °C)	0.02% SO_2, 10% H_2O	~75% (180 °C/3 h)	117
$Mn_{0.6}$/$Ce_{0.5}$–$Zr_{0.5}$–O	Impregnation/500 °C/6 h	0.06% NO, 0.06% NH_3, 3% O_2/30 000 h^{-1}	>90% (140–180 °C)	0.01% SO_2, 3% H_2O	~90% (180 °C/3 h)	139
$Mn_{0.4}$–$Ce_{0.07}$–Ti_1–O	Sol–gel/500 °C/6 h	0.1% NO, 0.1% NH_3, 3% O_2/40 000 h^{-1}	~100% (120–220 °C)	0.01% SO_2, 3% H_2O	~82% (150 °C/7 h)	140
$Mn_{0.4}$–$Ce_{0.5}$–$W_{0.1}$–O	Sol–gel/600 °C/3 h	0.05% NO, 0.05% NH_3, 5% O_2/40 000 h^{-1}	>80% (140–300 °C)	0.006% SO_2, 5% H_2O	~55% (150 °C/3 h)	141
$Mn_{0.3}$–$Ce_{0.7}$–O	Citric acid/650 °C/6 h	0.1% NO, 0.1% NH_3, 2% O_2/42 000 h^{-1}	~100% (120–150 °C)	0.01% SO_2, 6% H_2O	~92% (120 °C/4 h)	23
$Mn_{0.2}$–$Ce_{0.1}$–$Ti_{0.7}$–O	Hydrothermal/500 °C/6 h	0.05% NO, 0.05% NH_3, 5% O_2/64 000 h^{-1}	>95% (150–350 °C)	0.005% SO_2, 5% H_2O	~90% (200 °C/10 h)	96
Mn–Ce–W–Ti–O	Impregnation/400 °C/4 h	0.02% NO, 0.02% NH_3, 8% O_2/30 000 h^{-1}	~100% (160–200 °C)	0.01% SO_2, 8% H_2O	~85% (180 °C/10 h)	97
$Mn_{0.4}$–$Ce_{0.07}$–Ti_1–O	Co-precipitation/400 °C/2 h	0.06% NO, 0.06% NH_3, 3% O_2/40 000 h^{-1}	>92% (120–180 °C)	0.07% SO_2, 3% H_2O	61% (120 °C/2.5 h)	142
$Mn_{0.2}$–$Fe_{0.15}$–$Ce_{0.3}$–Ti_1–O	Sol–gel/500 °C/6 h	0.06% NO, 0.06% NH_3, 3% O_2/50 000 h^{-1}	>95% (160–260 °C)	0.01% SO_2, 3% H_2O	~85% (180 °C/6 h)	143
$Mn_{0.6}$–$Ce_{0.5}$–$Zr_{0.5}$–O	Impregnation/500 °C/6 h	0.06% NO, 0.066% NH_3, 6% O_2/45 000 h^{-1}	>95% (140–220 °C)	0.01% SO_2, 3% H_2O	~90% (180 °C/7 h)	144
$Mn_{0.4}$–$Fe_{0.1}$–$Ce_{0.5}$–O	Co-precipitation/500 °C/6 h	0.1% NO, 0.1% NH_3, 2% O_2/84 000 h^{-1}	>82% (150–180 °C)	0.01% SO_2, 2.5% H_2O	>90% (150 °C/4 h)	27
$Mn_{0.4}$–$Ce_{0.1}$–Ti_1–O	Sol–gel/500 °C/6 h	0.08% NO, 0.08% NH_3, 3% O_2/40 000 h^{-1}	~100% (150 °C)	0.01% SO_2, 3% H_2O	~60% (150 °C/10 h)	25
$Mn_{0.6}$–$Fe_{0.4}$–O	Citric acid/500 °C/3 h	0.1% NO, 0.1% NH_3, 3% O_2/30 000 h^{-1}	>95% (90–220 °C)	0.01% SO_2, 5% H_2O	~88% (120 °C/6 h)	98
10% Mn/Fe–Ti spinel	Impregnation/500 °C/3 h	0.05% NO, 0.05% NH_3, 2% O_2/24 000 cm^3 g^{-1} h^{-1}	>95% (150–250 °C)	0.006% SO_2, 8% H_2O	~80% (200 °C/13 h)	53
$Mn_{0.4}$–$Fe_{0.1}$/Ti_1–$Zr_{0.5}$–O	Sol–gel/500 °C/6 h	0.1% NO, 0.1% NH_3, 4% O_2/30 000 h^{-1}	>95% (80–180 °C)	0.01% SO_2, 8% H_2O	~70% (150 °C/5 h)	89
$Mn_{0.4}$–$Fe_{0.1}$/$Ti_{0.5}$–O	Sol–gel/500 °C/6 h	0.1% NO, 0.1% NH_3, 3% O_2/30 000 h^{-1}	~100% (150 °C)	0.02% SO_2	~65% (150 °C/6 h)	123
$Mn_{0.6}$–Ti_1–O	Sol–gel/500 °C/6 h	0.1% NO, 0.1% NH_3, 3% O_2/30 000 h^{-1}	~100% (110 °C)	0.003% SO_2	~85% (120 °C/9 h)	132
$Mn_{0.4}$–Ti_1–O	Sol–gel/500 °C/6 h	0.1% NO, 0.1% NH_3, 3% O_2/30 000 h^{-1}	>90% (180–250 °C)	0.02% SO_2, 3% H_2O	~70% (150 °C/6 h)	118
Mn–Fe–Ce–Ti–O	Sol–gel/500 °C/6 h	0.06% NO, 0.048% NH_3, 2% O_2/24 000 h^{-1}	>80% (200–300 °C)	0.03% SO_2, 10% H_2O	~80% (240 °C/5 h)	111
7% Mn/Ti_1–graphene	Impregnation/450° C/6 h	0.05% NO, 0.05% NH_3, 7% O_2/67 000 h^{-1}	>80% (120–180 °C)	0.02% SO_2, 10% H_2O	~72% (180 °C/3 h)	115
$Mn_{0.5}$–$Zr_{0.5}$–O	Citric acid/450 °C/3 h	0.1% NO, 0.1% NH_3, 3% O_2/30 000 h^{-1}	~100% (100–200 °C)	0.01% SO_2, 5% H_2O	~40% (150 °C/13 h)	124
$Mn_{2.5}$–$Cu_{0.1}$–Ti_1–O	Co-precipitation/350 °C/6 h	0.05% NO, 0.05% NH_3, 5% O_2/30 000 h^{-1}	~100% (60–280 °C)	0.01% SO_2, 11% H_2O	~60% (125 °C/10 h)	39
Mn_4/$Co_{0.6}$–$Ce_{2.7}$–$Zr_{2.7}$	Impregnation/500 °C/6 h	0.06% NO, 0.06% NH_3, 6% O_2/45 000 h^{-1}	>97% (120–220 °C)	0.01% SO_2, 3% H_2O	~93% (180 °C/7 h)	109
$Mn_{0.6}$–$Cr_{0.4}$–O	Citric acid/650 °C/3 h	0.1% NO, 0.1% NH_3, 3% O_2/30 000 h^{-1}	~100% (120–220 °C)	0.01% SO_2	~82% (120 °C/5 h)	37
$Mn_{0.3}$–$Ce_{0.7}$–O	Citric acid/650 °C/6 h	0.05% NO, 0.05% NH_3, 2% O_2/30 000 cm^3 g^{-1} h^{-1}	>95% (120–160 °C)	5% H_2O	~70% (120–140 °C)	61
$Mn_{0.3}$–$Ce_{0.7}$–O	Citric acid/650 °C/6 h	0.05% NO, 0.05% NH_3, 2% O_2/120 000 cm^3 g^{-1} h^{-1}	>90% (140–200 °C)	5% H_2O	>70% (160–200 °C)	88
Mn–Ce/W–Zr–O	Impregnation/550 °C/3 h	0.1% NO, 0.1% NH_3, 5% O_2/10 000 h^{-1}	>90% (150–250 °C)	0.01% SO_2, 10% H_2O	<80% (140–240 °C)	145
Mn–Ce/activated carbon honeycomb	Impregnation/400 °C/3 h	0.05% NO, 0.05% NH_3, 5% O_2/1910 h^{-1}	~84% (160 °C)	0.03% SO_2	~44% (160 °C/7 h)	113
$Mn_{0.23}$–$Nb_{0.23}$–$Ce_{0.54}$–O	Co-precipitation/650 °C/5 h	0.1% NO, 0.1% NH_3, 10% O_2/52 000 h^{-1}	—	5% H_2O	>80% (200–300 °C)	146
$Mn_{0.23}$–$Nb_{0.23}$–$Ce_{0.54}$–O	Co-precipitation/650 °C/5 h	0.1% NO, 0.1% NH_3, 10% O_2/52 000 h^{-1}	>78% (200–300 °C)	0.005% SO_2, 5% H_2O	~20% (250 °C/0.5 h)	147
$Mn_{2.5}$–$La_{2.5}$–Ce_1–Ni_1	500 °C/6 h	0.06% NO, 0.06% NH_3, 6% O_2/20 000 h^{-1}	~98% (150–350 °C)	0.03% SO_2	~85% (200 °C/4 h)	148

[a] Preparation process means of preparation method, calcination temperature and time. [b] Reaction gas mixture and GHSV. [c] NO conversion at a specified temperature. [d] The concentration of SO_2 and H_2O introduced on the basis of reaction gas. [e] NO conversion at a certain temperature after introducing SO_2 and/or H_2O for a specified time.

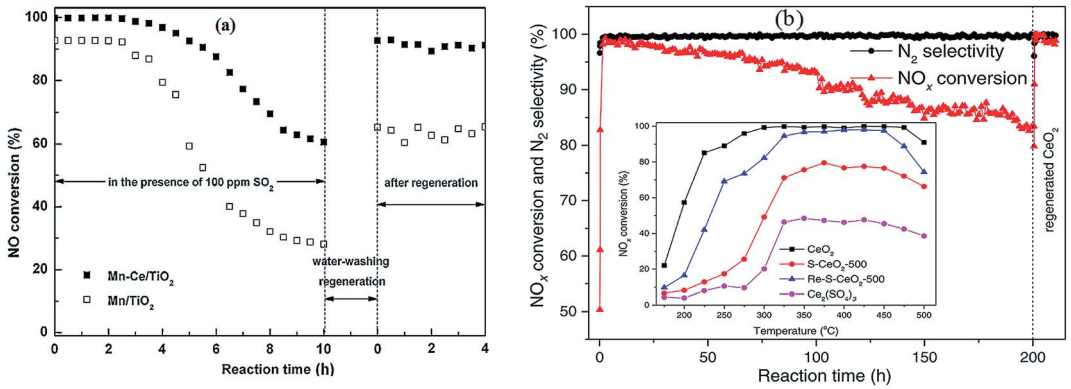

Fig. 9 SCR activities of Mn/Ti and Mn–Ce/Ti in the presence of SO_2. (a) Reaction conditions: [NO] = [NH_3] = 800 ppm, [O_2] = 3%, [SO_2] = 100 ppm, [H_2O] = 3 vol%, balance N_2, temperature: 150 °C, GHSV = 40 000 h^{-1}. (Reprinted from ref. 25. Copyright 2013, with permission from Elsevier.) (b) Regeneration of sulfur poisoned CeO_2 catalyst using a thermal treatment. Reaction conditions: [NO] = [NH_3] = 500 ppm, [O_2] = 5%, [SO_2] = 25 ppm, balance N_2, temperature: 350 °C, GHSV = 175 000 h^{-1}. (Reprinted from ref. 129. Copyright 2016, with permission from Elsevier.)

as in the cement production process. Alkali salts are important components in fine fly ash, which not only plugs the pores of catalysts, but also decreases SCR activity by reacting with the active phase.[154–156] In addition, because of the water solubility or ion exchange, alkali metal has a high liquidity to neutralize the acid sites.[157] For the traditional V_2O_5-based SCR catalysts, alkali metal deactivated these by affecting the acid sites on the surface.[154,158] Alkali metals could lower MnO_x reducibility, decrease specific surface areas and damage the acid sites of low temperature catalysts.

Zhou *et al.*[159] reported that sodium sulfate, used to simulate the combined effects of alkali metal and SO_2 in the flue gas, had strong effects on the activity of the Mn–Ce/TiO_2 catalyst, such as simultaneous pore occlusion and sulfation effect. Guo *et al.*[160] investigated the deactivation effect of sodium (Na) and potassium (K) on a Mn/TiO_2 catalyst. The catalyst was prepared using a sol–gel method and Na and K were doped *via* an impregnation method. The Mn/TiO_2 catalysts exhibited a high activity of 90% NO conversion. However, when Na or K was doped, the conversion was decreased from 95% to 78% and 27%, respectively. In this study, the effect of K was apparently more serious than that of Na.[161] Furthermore, Chen *et al.*[155] found that on the catalysts' surface chemisorbed oxygen was reduced by alkali and alkaline earth ions together with a decrease of SCR activity. The downward trend was K > Na > Ca > Mg.

Shen *et al.*[162,163] studied the effects of K, Na and Ca on a Mn–Ce/Zr catalyst. From the NH_3-TPD measurements, the adsorption of NH_3 was decreased when the catalyst was doped with alkali metal ions. This may indicate that the alkali metal on the surface of the catalysts may destroy the surface acidic sites, and decrease the redox property and chemisorbed oxygen. Furthermore, they also found that K was more harmful to the catalyst compared to Na or Ca. However, Kustov *et al.*[164] found that V_2O_5 supported on sulfated zirconium dioxide showed a good resistance towards alkali ions. Chen *et al.*[70] reported that the K resistance of the Mn/TiO_2 catalyst could be improved by doping it with Co, which increased the adsorption of NH_3 and NO_x species.

3.3 Heavy metal ions

Heavy metal ions, regarded as hazardous pollutants, can deactivate the SCR catalysts. Heavy metal ions in the flue gas are mainly generated from coal used as fuel.[165] It has been proved that heavy metals could lead to the deactivation of vanadium-based SCR catalysts.[166] Kong *et al.*[167] found that the Brønsted acid sites of a V–W/TiO_2 catalyst were impacted when mercury chloride was introduced. Actually, there is little heavy metal ions found in the downstream of the precipitator because the heavy metal ions usually exist in the fly ash. Moreover, water

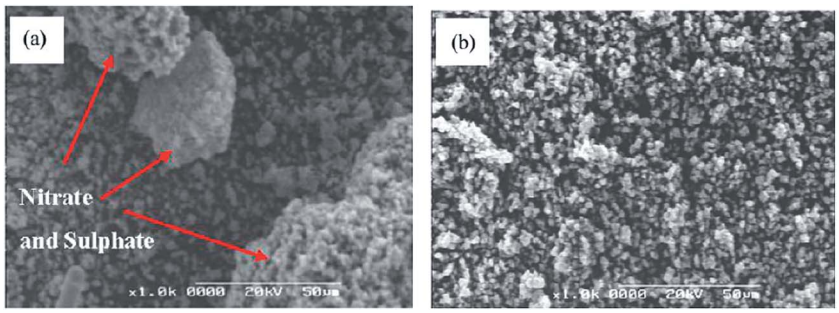

Fig. 10 SEM images (a) feeding with 400 ppm SO_2 at 150 °C for 26 h, (b) calcined at 200 °C and 400 °C for 2 h. (Reprinted from ref. 153. Copyright 2011, with permission from Elsevier.)

vapor exists in the flue gas all along. For the water solubility of heavy metal ions, it is necessary to take the effect of heavy metals into consideration.

Lead (Pb) and zinc (Zn) are typical heavy metals found in the flue gas of coal fired power plants. Guo *et al.*[156,168] and Li *et al.*[169] compared the poisoning effect of Pb and Zn on a Mn/TiO_2 catalyst. The Pb or Zn was loaded on to the Mn/TiO_2 catalyst using impregnation. As a result, both Pb and Zn were found to have a negative effect on the Mn/TiO_2 catalyst (Fig. 11a). From the characterization experiments, the redox ability of Zn–Mn/TiO_2 and Pb–Mn/TiO_2 was found to be decreased because of the drop of Mn^{4+} and chemisorbed oxygen. Zhou *et al.*[170] investigated the deactivation effects of lead(II) oxide (PbO) on the Mn–Ce/TiO_2 catalyst. It was proposed that the surface area, the concentration of Mn^{4+}, Ce^{3+} and chemisorbed oxygen was decreased after introducing PbO. Consequently, the performance of the Mn–Ce/TiO_2 catalyst was greatly decreased because of the poisoning of PbO (Fig. 11b).

Mercury (Hg^0) is a toxic trace element in the atmosphere and has a high concentration in coals used in China, such as anthracite, bituminous coal and lignite.[171] Researchers have attempted to remove the NO and Hg^0 simultaneously. However, Hg^0 is harmful to the catalysts of SCR of NO because it will compete with NH_3 for adsorption on the active sites.[172] Xu *et al.*[41] investigated the influence of Hg^0 on the NO conversion over a $LaMnO_3$ catalyst. The NO conversion had a slight decrease in the presence of Hg^0 (Fig. 12).

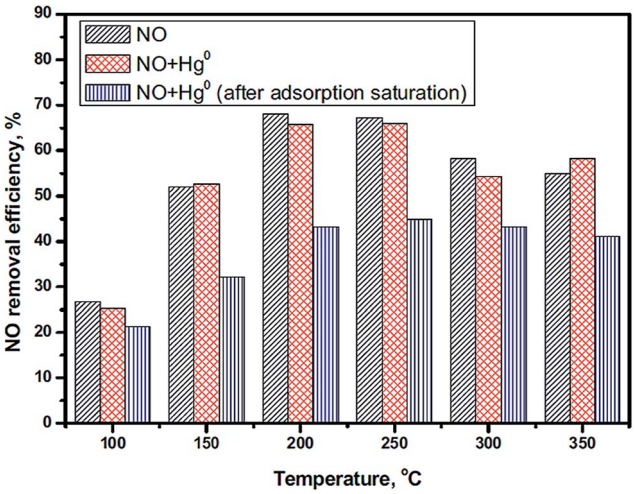

Fig. 12 The effect of Hg^0 on NO conversion. Reaction conditions: [NO] = [NH_3] = 500 ppm, [Hg^0] = 500 μg m^{-3}, [O_2] = 4%, balance N_2, GHSV = 478 000 h^{-1}. (Reprinted from ref. 41. Copyright 2016, with permission from Elsevier.)

4. Conclusions and perspectives

NH_3-SCR of NO_x in the presence of O_2 is one of the important strategies in controlling NO_x emissions. Low temperature SCR has been investigated for several decades. Mn-containing metal oxide catalysts generally gave the preferable performance. SCR of NO_x with NH_3 follows both the L–H and the E–R mechanisms. There is quite a similarity between these two different mechanisms. A comproportionation occurs in both the L–H and E–R mechanisms. Fast SCR has a higher reaction rate than standard SCR and it depends on the formation of NO_2. N_2O formation can mainly be explained using the E–R mechanism. A synergistic mechanism is vital for designing a remarkable metal oxide catalyst. Multi-metal cations will promote the performance mutually. Manganese cations mainly serve as the adsorption center for nitrogen. Thus, it is necessary to introduce an element for the adsorption of oxygen and to provide a redox cycle.

A big challenge in the industrial use of Mn-containing oxide catalysts is their durability. They are vulnerable to the effects of both SO_2 and H_2O. Sulfur oxides and water vapor cause the deactivation of Mn-containing catalysts. Alkali metals could lower manganese oxide reducibility, decrease specific surface areas and damage the acid sites of low temperature catalysts. The poisoning process of SO_2 can be classified into two categories: deposition of $(NH_4)_2SO_4$ and sulfation of the active phase. For the low temperature downstream of the flue gas, the deposition of $(NH_4)_2SO_4$ or NH_4HSO_4 occurs more easily and NH_3 is evidently adsorbed by H_2O in comparison with the

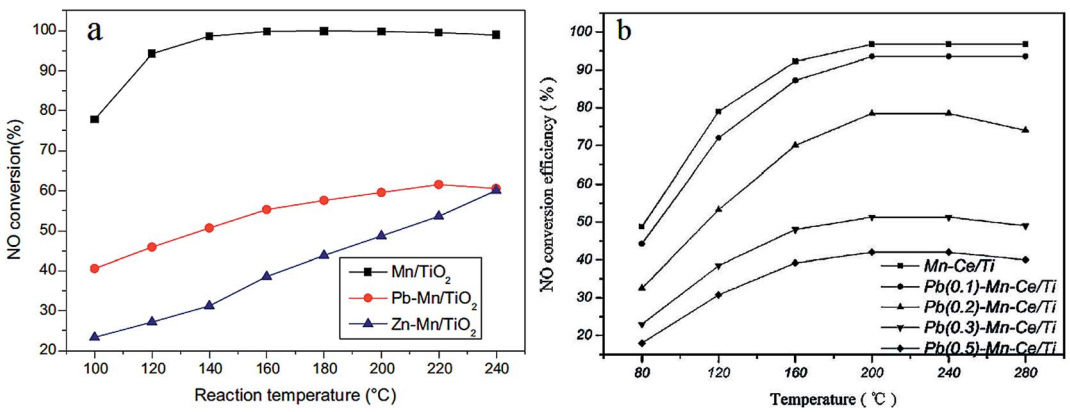

Fig. 11 NO conversion over pure and poisoned catalysts. (a) Reaction conditions: [NO] = [NH_3] = 600 ppm, [O_2] = 5%, balance N_2, GHSV = 108 000 h^{-1}. (Reprinted from ref. 156. Copyright 2015, with permission from Elsevier.) (b) Reaction conditions: [NO] = [NH_3] = 800 ppm, [O_2] = 5%, balance N_2, GHSV = 200 000 h^{-1}. (Reprinted from ref. 170. Copyright 2016, with permission from Elsevier.)

operation upstream. Many efforts have been made to improve the durability. Nonetheless, few techniques have been useful in practical industrial applications.

On the basis of the previous analysis, some conclusions can be drawn as follows:

(1) Most research is related to the performance of the catalysts, such as NO conversion, N_2 selectivity and poisons' tolerance, as well as the mechanism of this process. An excellent NO conversion of catalysts has been obtained, however, the N_2 selectivity is not satisfactory.

(2) Less effort has been made on determining the relationship of metal oxide crystal structure and its performance, which is required for the design of catalysts. More attention should be given to the relationship between the catalysts' structure and its reaction mechanism, which guides us exactly to design a low temperature SCR catalyst for different flue gases.

(3) Mn-containing metal oxide catalysts show a notable SCR performance at low temperature. However, the single manganese oxide catalysts have a poor tolerance of SO_2 and H_2O, which has been improved by modifying other elements in bench scale experiments. Researchers have been engaged in improving Mn-containing catalysts by modifying them with different metal oxides. Ce can enhance the adsorption of NO and O_2 which benefits the oxidization of NO to NO_2 and improves sulfur resistance, and inhibits the formation of $(NH_4)_2SO_4$ and NH_4HSO_4. Ce has good selectivity for improving the catalysts' performance. More research efforts should be made on the activity and poisoning tolerance.

(4) Most catalysts were powder rather than monolith catalysts, such as honeycomb or slab. A laboratory study is a small scale test that will react differently to industrial tests. Specific surface area is important to the activity and closely related to the particles' size, shape and aggregation. The preparation method is also important to the catalysts' performance. Researchers should give more attention to pilot scale tests or industrial tests.

(5) The low temperature SCR catalysts have been investigated for several decades. Lots of elements have been studied in the catalysts. To avoid repetitive work and waste of resources, a low temperature SCR catalysts' materials database should be built.

(6) Heaps of disabled SCR catalysts should be regenerated and reused. The regeneration and recycling of SCR catalysts is another big task for researchers. This problem should be taken into consideration while researchers are designing new SCR catalysts.

Acknowledgements

This work was sponsored by the National Natural Science Foundation of China (Grants U1360202, 51472030, 51672024 and 51502014) and the 111 Project (No. B17003). The authors would like to thank the editor for editing the manuscript and the anonymous reviewers for their detailed and helpful comments.

References

1 H. Amini, S.-M. Taghavi-Shahri, S. B. Henderson, V. Hosseini, H. Hassankhany, M. Naderi, S. Ahadi, C. Schindler, N. Künzli and M. Yunesian, *Sci. Rep.*, 2016, **6**, 32970.
2 A. Richter, J. P. Burrows, H. Nusz, C. Granier and U. Niemeier, *Nature*, 2005, **437**, 129–132.
3 J. N. Galloway, F. J. Dentener, D. G. Capone, E. W. Boyer, R. W. Howarth, S. P. Seitzinger, G. P. Asner, C. C. Cleveland, P. A. Green, E. A. Holland, D. M. Karl, A. F. Michaels, J. H. Porter, A. R. Townsend and C. J. Vöosmarty, *Biogeochemistry*, 2004, **70**, 153–226.
4 J. Zhu and A. Thomas, *Appl. Catal., B*, 2009, **92**, 225–233.
5 M. Fu, C. Li, P. Lu, L. Qu, M. Zhang, Y. Zhou, M. Yu and Y. Fang, *Catal. Sci. Technol.*, 2014, **4**, 14–25.
6 C. Tang, H. Zhang and L. Dong, *Catal. Sci. Technol.*, 2016, **6**, 1248–1264.
7 B. Liu, Y. H. Wang and H. Xu, *J. Energy Eng.*, 2016, **142**, 10.
8 B. Liu, B. Bao, Y. Wang and H. Xu, *J. Energy Inst.*, 2016, **90**, 441–451.
9 T. Ishihara, *J. Catal.*, 2003, **220**, 104–114.
10 D. G. Streets and S. T. Waldhoff, *Atmos. Environ.*, 2000, **34**, 363–374.
11 P. Forzatti, *Appl. Catal., A*, 2001, **222**, 221–236.
12 M. Koebel, G. Madia and M. Elsener, *Catal. Today*, 2002, **73**, 239–247.
13 M. T. Javed, N. Irfan and B. M. Gibbs, *J. Environ. Manage.*, 2007, **83**, 251–289.
14 S. W. Bae, S. A. Roh and S. D. Kim, *Chemosphere*, 2006, **65**, 170–175.
15 J. O. L. Wendt, W. P. Linak, P. W. Groff and R. K. Srivastava, *AIChE J.*, 2001, **47**, 2603–2617.
16 S. Roy and A. Baiker, *Chem. Rev.*, 2009, **109**, 4054–4091.
17 G. Busca, L. Lietti, G. Ramis and F. Berti, *Appl. Catal., B*, 1998, **18**, 1–36.
18 K.-I. Shimizu, J. Shibata, H. Yoshida, A. Satsuma and T. Hattori, *Appl. Catal., B*, 2001, **30**, 151–162.
19 S. Brandenberger, O. Kroecher, A. Tissler and R. Althoff, *Catal. Rev.: Sci. Eng.*, 2008, **50**, 492–531.
20 L. Casagrande, L. Lietti, I. Nova, P. Forzatti and A. Baiker, *Appl. Catal., B*, 1999, **22**, 63–67.
21 K. Bourikas, C. Fountzoula and C. Kordulis, *Appl. Catal., B*, 2004, **52**, 145–153.
22 S. Hodjati, K. Vaezzadeh, C. Petit, V. Pitchon and A. Kiennemann, *Top. Catal.*, 2001, **16**, 151–155.
23 G. Qi and R. T. Yang, *Chem. Commun.*, 2003, 848–849, DOI: 10.1039/b212725c.
24 R. Qu, X. Gao, K. Cen and J. Li, *Appl. Catal., B*, 2013, **142–143**, 290–297.
25 R. Jin, Y. Liu, Y. Wang, W. Cen, Z. Wu, H. Wang and X. Weng, *Appl. Catal., B*, 2014, **148–149**, 582–588.
26 D. A. Peña, B. S. Uphade and P. G. Smirniotis, *J. Catal.*, 2004, **221**, 421–431.
27 G. Qi, R. T. Yang and R. Chang, *Appl. Catal., B*, 2004, **51**, 93–106.
28 B. Thirupathi and P. G. Smirniotis, *Appl. Catal., B*, 2011, **110**, 195–206.
29 W. Shan, F. Liu, H. He, X. Shi and C. Zhang, *Appl. Catal., B*, 2012, **115**, 100–106.

30 N. Apostolescu, B. Geiger, K. Hizbullah, M. T. Jan, S. Kureti, D. Reichert, F. Schott and W. Weisweiler, *Appl. Catal., B*, 2006, **62**, 104–114.
31 F. Kapteijn, L. Singoredjo, A. Andreini and J. A. Moulijn, *Appl. Catal., B*, 1994, **3**, 173–189.
32 F. ç. Larachi, J. Pierre, A. Adnot and A. Bernis, *Appl. Surf. Sci.*, 2002, **195**, 236–250.
33 B. Shen, F. Wang and T. Liu, *Powder Technol.*, 2014, **253**, 152–157.
34 F. Liu, H. He, C. Zhang, Z. Feng, L. Zheng, Y. Xie and T. Hu, *Appl. Catal., B*, 2010, **96**, 408–420.
35 S. Yang, S. Xiong, Y. Liao, X. Xiao, F. Qi, Y. Peng, Y. Fu, W. Shan and J. Li, *Environ. Sci. Technol.*, 2014, **48**, 10354–10362.
36 H. Hu, S. Cai, H. Li, L. Huang, L. Shi and D. Zhang, *ACS Catal.*, 2015, **5**, 6069–6077.
37 Z. Chen, Q. Yang, H. Li, X. Li, L. Wang and S. Chi Tsang, *J. Catal.*, 2010, **276**, 56–65.
38 M. A. Zamudio, N. Russo and D. Fino, *Ind. Eng. Chem. Res.*, 2011, **50**, 6668–6672.
39 M. Kang, E. D. Park, J. M. Kim and J. E. Yie, *Catal. Today*, 2006, **111**, 236–241.
40 D. Fang, J. Xie, D. Mei, Y. Zhang, F. He, X. Liu and Y. Li, *RSC Adv.*, 2014, **4**, 25540.
41 H. Xu, Z. Qu, C. Zong, F. Quan, J. Mei and N. Yan, *Appl. Catal., B*, 2016, **186**, 30–40.
42 Z. Liu and S. Ihl Woo, *Catal. Rev.*, 2006, **48**, 43–89.
43 J. Li, H. Chang, L. Ma, J. Hao and R. T. Yang, *Catal. Today*, 2011, **175**, 147–156.
44 C. Liu, J.-W. Shi, C. Gao and C. Niu, *Appl. Catal., A*, 2016, **522**, 54–69.
45 http://www.sdpc.gov.cn/gzdt/201409/t20140919_626240.html, accessed Dec. 7th, 2016.
46 P. R. Ettireddy, N. Ettireddy, T. Boningari, R. Pardemann and P. G. Smirniotis, *J. Catal.*, 2012, **292**, 53–63.
47 G. Busca, M. A. Larrubia, L. Arrighi and G. Ramis, *Catal. Today*, 2005, **107–108**, 139–148.
48 G. Zhou, B. Zhong, W. Wang, X. Guan, B. Huang, D. Ye and H. Wu, *Catal. Today*, 2011, **175**, 157–163.
49 L. Qiu, J. Meng, D. Pang, C. Zhang and F. Ouyang, *Catal. Lett.*, 2015, **145**, 1500–1509.
50 D. Ye, *Practical Inorganic Thermodynamic Data Manual*, Metallurgical Industry Press, Beijing, 1st edn, 1981.
51 I. Nam, *J. Catal.*, 1989, **119**, 269.
52 S. Yang, F. Qi, Y. Liao, S. Xiong, Y. Lan, Y. Fu, W. Shan and J. Li, *Ind. Eng. Chem. Res.*, 2014, **53**, 5810–5819.
53 S. Yang, F. Qi, S. Xiong, H. Dang, Y. Liao, P. K. Wong and J. Li, *Appl. Catal., B*, 2016, **181**, 570–580.
54 T. Chen, B. Guan, H. Lin and L. Zhu, *Chin. J. Catal.*, 2014, **35**, 294–301.
55 S. Yang, C. Wang, J. Li, N. Yan, L. Ma and H. Chang, *Appl. Catal., B*, 2011, **110**, 71–80.
56 G. Qi and R. T. Yang, *J. Phys. Chem. B*, 2004, **108**, 15738–15747.
57 F. Liu and H. He, *Catal. Today*, 2010, **153**, 70–76.
58 Z. Wu, B. Jiang, Y. Liu, H. Wang and R. Jin, *Environ. Sci. Technol.*, 2007, **41**, 5812–5817.
59 D. Fang, F. He, D. Li and J. Xie, *Appl. Surf. Sci.*, 2013, **285**, 215–219.
60 D. Fang, J. Xie, H. Hu, H. Yang, F. He and Z. Fu, *Chem. Eng. J.*, 2015, **271**, 23–30.
61 S. Xiong, Y. Liao, X. Xiao, H. Dang and S. Yang, *J. Phys. Chem. C*, 2015, **119**, 4180–4187.
62 F. Eigenmann, M. Maciejewski and A. Baiker, *Appl. Catal., B*, 2006, **62**, 311–318.
63 X. Tang, J. Li, L. Sun and J. Hao, *Appl. Catal., B*, 2010, **99**, 156–162.
64 I. Nova, C. Ciardelli, E. Tronconi, D. Chatterjee and B. Bandl-Konrad, *Catal. Today*, 2006, **114**, 3–12.
65 M. Koebel, G. Madia, F. Raimondi and A. Wokaun, *J. Catal.*, 2002, **209**, 159–165.
66 M. Koebel, M. Elsener and G. Madia, *Ind. Eng. Chem. Res.*, 2001, **40**, 52–59.
67 G. Madia, M. Koebel, M. Elsener and A. Wokaun, *Ind. Eng. Chem. Res.*, 2002, **41**, 3512–3517.
68 M. Stanciulescu, P. Bulsink, G. Caravaggio, L. Nossova and R. Burich, *Appl. Surf. Sci.*, 2014, **300**, 201–207.
69 W. Zhao, C. Li, P. Lu, Q. Wen, Y. Zhao, X. Zhang, C. Fan and S. Tao, *Environ. Technol.*, 2013, **34**, 81–90.
70 Q.-L. Chen, R.-T. Guo, Q.-S. Wang, W.-G. Pan, N.-Z. Yang, C.-Z. Lu and S.-X. Wang, *J. Taiwan Inst. Chem. Eng.*, 2016, **64**, 116–123.
71 X. Zeng, X. Huo, T. Zhu, X. Hong and Y. Sun, *Molecules*, 2016, **21**, 1491.
72 Y. Liang, Y. Huang, H. Zhang, L. Lan, M. Zhao, M. Gong, Y. Chen and J. Wang, *Environ. Sci. Pollut. Res. Int.*, 2017, **24**, 9314–9324.
73 A. Grossale, I. Nova and E. Tronconi, *J. Catal.*, 2009, **265**, 141–147.
74 L. Zhu, Z. Zhong, H. Yang and C. Wang, *Water, Air, Soil Pollut.*, 2016, **227**, 476.
75 A. Grossale, I. Nova, E. Tronconi, D. Chatterjee and M. Weibel, *J. Catal.*, 2008, **256**, 312–322.
76 G. Qi and R. T. Yang, *J. Catal.*, 2003, **217**, 434–441.
77 R. Q. Long, R. T. Yang and R. Chang, *Chem. Commun.*, 2002, 452–453, DOI: 10.1039/b111382h.
78 L. J. France, Q. Yang, W. Li, Z. Chen, J. Guang, D. Guo, L. Wang and X. Li, *Appl. Catal., B*, 2017, **206**, 203–215.
79 Y. Zhu, Y. Zhang, R. Xiao, T. Huang and K. Shen, *Catal. Commun.*, 2017, **88**, 64–67.
80 S. M. Mousavi, A. Niaei, M. J. Illán Gómez, D. Salari, P. Nakhostin Panahi and V. Abaladejo-Fuentes, *Mater. Chem. Phys.*, 2014, **143**, 921–928.
81 T. Wang, K. Sun, Z. Lu and Y. Zhang, *React. Kinet., Mech. Catal.*, 2010, **101**, 153–161.
82 Y. Liu, T. Gu, X. Weng, Y. Wang, Z. Wu and H. Wang, *J. Phys. Chem. C*, 2012, **116**, 16582–16592.
83 S. Xiong, Y. Liao, H. Dang, F. Qi and S. Yang, *RSC Adv.*, 2015, **5**, 27785–27793.
84 L. Xu, X.-S. Li, M. Crocker, Z.-S. Zhang, A.-M. Zhu and C. Shi, *J. Mol. Catal. A: Chem.*, 2013, **378**, 82–90.
85 B. Jiang, Z. Li and S.-C. Lee, *Chem. Eng. J.*, 2013, **225**, 52–58.
86 S. Suarez, J. Martin, M. Yates, P. Avila and J. Blanco, *J. Catal.*, 2005, **229**, 227–236.

87 M. A. Zamudio, N. Russo and D. Fino, *Ind. Eng. Chem. Res.*, 2011, **50**, 6668–6672.
88 S. Yang, Y. Liao, S. Xiong, F. Qi, H. Dang, X. Xiao and J. Li, *J. Phys. Chem. C*, 2014, **118**, 21500–21508.
89 B. Jiang, B. Deng, Z. Zhang, Z. Wu, X. Tang, S. Yao and H. Lu, *J. Phys. Chem. C*, 2014, **118**, 14866–14875.
90 T.-Y. Li, S.-J. Chiang, B.-J. Liaw and Y.-Z. Chen, *Appl. Catal., B*, 2011, **103**, 143–148.
91 R. Farra, M. García-Melchor, M. Eichelbaum, M. Hashagen, W. Frandsen, J. Allan, F. Girgsdies, L. Szentmiklósi, N. López and D. Teschner, *ACS Catal.*, 2013, **3**, 2256–2268.
92 S. Imamura, A. Doi and S. Ishida, *Ind. Eng. Chem. Prod. Res. Dev.*, 1985, **24**, 75–80.
93 D. A. Peña, B. S. Uphade, E. P. Reddy and P. G. Smirniotis, *J. Phys. Chem. B*, 2004, **108**, 9927–9936.
94 H. Chang, J. Li, J. Yuan, L. Chen, Y. Dai, H. Arandiyan, J. Xu and J. Hao, *Catal. Today*, 2013, **201**, 139–144.
95 R. Jin, Y. Liu, Z. Wu, H. Wang and T. Gu, *Chemosphere*, 2010, **78**, 1160–1166.
96 Z. Liu, J. Zhu, J. Li, L. Ma and S. I. Woo, *ACS Appl. Mater. Interfaces*, 2014, **6**, 14500–14508.
97 D. W. Kwon, K. B. Nam and S. C. Hong, *Appl. Catal., A*, 2015, **497**, 160–166.
98 Z. Chen, F. Wang, H. Li, Q. Yang, L. Wang and X. Li, *Ind. Eng. Chem. Res.*, 2012, **51**, 202–212.
99 Y. J. Kim, H. J. Kwon, I.-S. Nam, J. W. Choung, J. K. Kil, H.-J. Kim, M.-S. Cha and G. K. Yeo, *Catal. Today*, 2010, **151**, 244–250.
100 Z. Liu, Y. Liu, Y. Li, H. Su and L. Ma, *Chem. Eng. J.*, 2016, **283**, 1044–1050.
101 Z. Liu, Y. Li, T. Zhu, H. Su and J. Zhu, *Ind. Eng. Chem. Res.*, 2014, **53**, 12964–12970.
102 P. Lu, C. Li, G. Zeng, L. He, D. Peng, H. Cui, S. Li and Y. Zhai, *Appl. Catal., B*, 2010, **96**, 157–161.
103 Y. Shen, S. Zhu, T. Qiu and S. Shen, *Catal. Commun.*, 2009, **11**, 20–23.
104 G. Ramis, *J. Catal.*, 1990, **124**, 574–576.
105 G. Busca, *Appl. Catal., B*, 1998, **18**, 1–36.
106 P. R. Ettireddy, N. Ettireddy, S. Mamedov, P. Boolchand and P. G. Smirniotis, *Appl. Catal., B*, 2007, **76**, 123–134.
107 M. Inomata, *J. Catal.*, 1980, **62**, 140–148.
108 S. Xiong, Y. Liao, X. Xiao, H. Dang and S. Yang, *Catal. Sci. Technol.*, 2015, **5**, 2132–2140.
109 X. Zhang, B. Shen, K. Wang and J. Chen, *J. Ind. Eng. Chem.*, 2013, **19**, 1272–1279.
110 X. Wang, X. Li, Q. Zhao, W. Sun, M. Tade and S. Liu, *Chem. Eng. J.*, 2016, **288**, 216–222.
111 J. Yu, F. Guo, Y. Wang, J. Zhu, Y. Liu, F. Su, S. Gao and G. Xu, *Appl. Catal., B*, 2010, **95**, 160–168.
112 G. Xie, Z. Liu, Z. Zhu, Q. Liu, J. Ge and Z. Huang, *J. Catal.*, 2004, **224**, 36–41.
113 Y. Wang, X. Li, L. Zhan, C. Li, W. Qiao and L. Ling, *Ind. Eng. Chem. Res.*, 2015, **54**, 2274–2278.
114 Y.-J. Shi, H. Shu, Y.-H. Zhang, H.-M. Fan, Y.-P. Zhang and L.-J. Yang, *Fuel Process. Technol.*, 2016, **150**, 141–147.
115 X. Lu, C. Song, C.-C. Chang, Y. Teng, Z. Tong and X. Tang, *Ind. Eng. Chem. Res.*, 2014, **53**, 11601–11610.
116 D. Zhang, L. Zhang, L. Shi, C. Fang, H. Li, R. Gao, L. Huang and J. Zhang, *Nanoscale*, 2013, **5**, 1127–1136.
117 X. Lu, C. Song, S. Jia, Z. Tong, X. Tang and Y. Teng, *Chem. Eng. J.*, 2015, **260**, 776–784.
118 B. Jiang, Y. Liu and Z. Wu, *J. Hazard. Mater.*, 2009, **162**, 1249–1254.
119 Z. Zhu, Z. Liu, S. Liu and H. Niu, *Appl. Catal., B*, 2001, **30**, 267–276.
120 W. Q. Xu, H. He and Y. B. Yu, *J. Phys. Chem. C*, 2009, **113**, 4426–4432.
121 R. Q. Long and R. T. Yang, *J. Catal.*, 1999, **186**, 254–268.
122 H. H. Phil, M. P. Reddy, P. A. Kumar, L. K. Ju and J. S. Hyo, *Appl. Catal., B*, 2008, **78**, 301–308.
123 B. Q. Jiang, Z. B. Wu, Y. Liu, S. C. Lee and W. K. Ho, *J. Phys. Chem. C*, 2010, **114**, 4961–4965.
124 J. Zuo, Z. Chen, F. Wang, Y. Yu, L. Wang and X. Li, *Ind. Eng. Chem. Res.*, 2014, **53**, 2647–2655.
125 W. Sjoerd Kijlstra, M. Biervliet, E. K. Poels and A. Bliek, *Appl. Catal., B*, 1998, **16**, 327–337.
126 Z. Wu, R. Jin, H. Wang and Y. Liu, *Catal. Commun.*, 2009, **10**, 935–939.
127 Z. Liu, Y. Yi, S. Zhang, T. Zhu, J. Zhu and J. Wang, *Catal. Today*, 2013, **216**, 76–81.
128 L. Kylhammar, P.-A. Carlsson, H. H. Ingelsten, H. Grönbeck and M. Skoglundh, *Appl. Catal., B*, 2008, **84**, 268–276.
129 Y. Shi, S. Tan, X. Wang, M. Li, S. Li and W. Li, *Catal. Commun.*, 2016, **86**, 67–71.
130 H. Chang, X. Chen, J. Li, L. Ma, C. Wang, C. Liu, J. W. Schwank and J. Hao, *Environ. Sci. Technol.*, 2013, **47**, 5294–5301.
131 H. Chang, J. Li, X. Chen, L. Ma, S. Yang, J. W. Schwank and J. Hao, *Catal. Commun.*, 2012, **27**, 54–57.
132 Y. Shi, S. Chen, H. Sun, Y. Shu and X. Quan, *Catal. Commun.*, 2013, **42**, 10–13.
133 M. D. Amiridis, I. E. Wachs, G. Deo, J.-M. Jehng and D. S. Kim, *J. Catal.*, 1996, **161**, 247–253.
134 L. Chen, Z. Si, X. Wu, D. Weng and Z. Wu, *J. Environ. Sci.*, 2015, **31**, 240–247.
135 Z. Lei, B. Han, K. Yang and B. Chen, *Chem. Eng. J.*, 2013, **215–216**, 651–657.
136 S. Pan, H. Luo, L. Li, Z. Wei and B. Huang, *J. Mol. Catal. A: Chem.*, 2013, **377**, 154–161.
137 Z. Sheng, Y. Hu, J. Xue, X. Wang and W. Liao, *J. Rare Earths*, 2012, **30**, 676–682.
138 R. Jin, Y. Liu, Z. Wu, H. Wang and T. Gu, *Catal. Today*, 2010, **153**, 84–89.
139 B. Shen, Y. Wang, F. Wang and T. Liu, *Chem. Eng. J.*, 2014, **236**, 171–180.
140 Z. Wu, R. Jin, Y. Liu and H. Wang, *Catal. Commun.*, 2008, **9**, 2217–2220.
141 Z. Ma, X. Wu, Y. Feng, Z. Si and D. Weng, *Catal. Commun.*, 2015, **69**, 188–192.
142 Z. Sheng, Y. Hu, J. Xue, X. Wang and W. Liao, *Environ. Technol.*, 2012, **33**, 2421–2428.
143 B. Shen, T. Liu, N. Zhao, X. Yang and L. Deng, *J. Environ. Sci.*, 2010, **22**, 1447–1454.

144 B. Shen, X. Zhang, H. Ma, Y. Yao and T. Liu, *J. Environ. Sci.*, 2013, **25**, 791–800.
145 H. Xu, Q. Zhang, C. Qiu, T. Lin, M. Gong and Y. Chen, *Chem. Eng. Sci.*, 2012, **76**, 120–128.
146 M. Casapu, O. Kröcher, M. Mehring, M. Nachtegaal, C. Borca, M. Harfouche and D. Grolimund, *J. Phys. Chem. C*, 2010, **114**, 9791–9801.
147 M. Casapu, O. Kröcher and M. Elsener, *Appl. Catal., B*, 2009, **88**, 413–419.
148 B. Yang, D.-H. Zheng, Y.-S. Shen, Y.-S. Qiu, B. Li, Y.-W. Zeng, S.-B. Shen and S.-M. Zhu, *J. Ind. Eng. Chem.*, 2015, **24**, 148–152.
149 B. Yang, Y. Shen, S. Shen and S. Zhu, *J. Rare Earths*, 2013, **31**, 130–136.
150 Y. Yu, C. He, J. Chen, L. Yin, T. Qiu and X. Meng, *Catal. Commun.*, 2013, **39**, 78–81.
151 M. Pourkhalil, A. Z. Moghaddam, A. Rashidi, J. Towfighi and Y. Mortazavi, *Appl. Surf. Sci.*, 2013, **279**, 250–259.
152 J. Huang, Z. Tong, Y. Huang and J. Zhang, *Appl. Catal., B*, 2008, **78**, 309–314.
153 B. Guan, H. Lin, L. Zhu and Z. Huang, *J. Phys. Chem. C*, 2011, **115**, 12850–12863.
154 R. Khodayari and C. U. I. Odenbrand, *Appl. Catal., B*, 2001, **30**, 87–99.
155 L. Chen, J. Li and M. Ge, *Chem. Eng. J.*, 2011, **170**, 531–537.
156 R.-T. Guo, Q.-S. Wang, W.-G. Pan, Q.-L. Chen, H.-L. Ding, X.-F. Yin, N.-Z. Yang, C.-Z. Lu, S.-X. Wang and Y.-C. Yuan, *J. Mol. Catal. A: Chem.*, 2015, **407**, 1–7.
157 L. Zhang, S. Cui, H. Guo, X. Ma and X. Luo, *J. Mol. Catal. A: Chem.*, 2014, **390**, 14–21.
158 F. Moradi, J. Brandin, M. Sohrabi, M. Faghihi and M. Sanati, *Appl. Catal., B*, 2003, **46**, 65–76.
159 A. Zhou, D. Yu, L. Yang and Z. Sheng, *Appl. Surf. Sci.*, 2016, **378**, 167–173.
160 R.-T. Guo, Q.-S. Wang, W.-G. Pan, W.-L. Zhen, Q.-L. Chen, H.-L. Ding, N.-Z. Yang and C.-Z. Lu, *Appl. Surf. Sci.*, 2014, **317**, 111–116.
161 X. S. Du, X. Gao, R. Y. Qu, P. D. Ji, Z. Y. Luo and K. F. Cen, *Chemcatchem*, 2012, **4**, 2075–2081.
162 S. Boxiong, Y. Yan, C. Jianhong and Z. Xiaopeng, *Microporous Mesoporous Mater.*, 2013, **180**, 262–269.
163 B. Shen, L. Deng and J. Chen, *Front. Environ. Sci. Eng.*, 2013, **7**, 512–517.
164 A. L. Kustov, M. Y. Kustova, R. Fehrmann and P. Simonsen, *Appl. Catal., B*, 2005, **58**, 97–104.
165 R. Stolle, H. Koeser and H. Gutberlet, *Appl. Catal., B*, 2014, **144**, 486–497.
166 Y. Jiang, X. Gao, Y. Zhang, W. Wu, H. Song, Z. Luo and K. Cen, *J. Hazard. Mater.*, 2014, **274**, 270–278.
167 M. Kong, Q. Liu, L. Jiang, F. Guo, S. Ren, L. Yao and J. Yang, *Catal. Commun.*, 2016, **85**, 34–38.
168 R.-T. Guo, C.-Z. Lu, W.-G. Pan, W.-L. Zhen, Q.-S. Wang, Q.-L. Chen, H.-L. Ding and N.-Z. Yang, *Catal. Commun.*, 2015, **59**, 136–139.
169 W. Li, R.-T. Guo, S.-X. Wang, W.-G. Pan, Q.-L. Chen, M.-Y. Li, P. Sun and S.-M. Liu, *Fuel Process. Technol.*, 2016, **154**, 235–242.
170 L. Zhou, C. Li, L. Zhao, G. Zeng, L. Gao, Y. Wang and M. E. Yu, *Appl. Surf. Sci.*, 2016, **389**, 532–539.
171 C. Zhu, H. Tian, K. Cheng, K. Liu, K. Wang, S. Hua, J. Gao and J. Zhou, *J. Cleaner Prod.*, 2016, **114**, 343–351.
172 P. Wang, S. Su, J. Xiang, H. You, F. Cao, L. Sun, S. Hu and Y. Zhang, *Chemosphere*, 2014, **101**, 49–54.